

### III. 附錄 別刷



## Biochemical and Physiological Regulation of Cardiac Myocyte Contraction by Cardiac-Specific Myosin Light Chain Kinase

Osamu Tsukamoto, MD, PhD; Masafumi Kitakaze, MD, PhD

Cardiac-specific myosin light chain kinase (cMLCK) is the kinase predominantly responsible for the maintenance of the basal level of phosphorylation of cardiac myosin light chain 2 (MLC2), which it phosphorylates at Ser-15. This phosphorylation repels the myosin heads from the thick myosin filament and moves them toward the thin actin filament. Unlike smooth muscle cells, MLC2 phosphorylation in striated muscle cells appears to be a positive modulator of  $Ca^{2+}$  sensitivity that shifts the  $Ca^{2+}$ -force relationship toward the left and increases the maximal force response and thus does not initiate muscle contraction. Recent studies have revealed an increasing number of details of the biochemical, physiological, and pathophysiological characteristics of cMLCK. The combination of recent technological advances and the discovery of a novel class of biologically active nonstandard peptides will hopefully translate into the development of drugs for the treatment of heart diseases. (*Circ J* 2013; **77**: 2218–2225)

**Key Words:**  $Ca^{2+}$ /calmodulin; Muscle contraction; Myosin light chain kinase; Regulatory myosin light chain

Actin and myosin are essential for the generation of contractile force. In 1954, Huxley and Hanson proposed the “sliding filament theory”, which states that contractile force is generated through slippage of the cross-bridges between actin and myosin filaments<sup>1</sup> and that purified actin and myosin are not sufficient for active movement. In 1962, intracellular calcium ( $[Ca^{2+}]_i$ ) was identified as acting a trigger of muscle contraction.<sup>2</sup> Although force generation can be achieved with only myosin and actin, additional proteins are required for its regulation. In smooth muscle, an increase in  $[Ca^{2+}]_i$  induces the binding of  $Ca^{2+}$ /calmodulin to smooth muscle-specific myosin light chain kinase (smMLCK), which leads to the phosphorylation of cardiac myosin light chain 2 (MLC2) in thick myosin filaments, activation of the ATPase of myosin heads and initiation of muscle contraction.<sup>3</sup> Thus, smooth muscle cells use smMLCK as a  $[Ca^{2+}]_i$  sensor and initiator of muscle contraction<sup>4</sup> (Figure 1). In contrast, troponin is specifically expressed in skeletal and cardiac muscle cells and works as a sensing protein of  $[Ca^{2+}]_i$ .<sup>5</sup> In contrast to smooth muscle cells, the initiation of striated muscle contraction is regulated primarily by the troponin-tropomyosin complex in thin actin filaments and not through MLC2 phosphorylation. The binding of  $Ca^{2+}$  to troponin C leads to relief of the inhibition of the binding of cross-bridges to thin actin filaments, and this relief triggers striated muscle contraction (Figure 1). However, endogenous expression of troponin proteins in smooth muscle cells was reported recently,<sup>6</sup> although the physiological role of the troponin complex in the regulation of

smooth muscle contraction still remains unknown.

Following the discovery of smMLCK and skeletal muscle MLCK (skMLCK), a third MLCK, named cardiac MLCK (cMLCK), was identified in 2007<sup>7</sup> and is expressed exclusively in cardiac myocytes. However, what is the role of MLCK in striated muscle cells? Because both skeletal and cardiac muscle cells express specific MLCKs (ie, skMLCK and cMLCK, respectively), MLCKs might play specific physiological roles in each cell type.

### Intracellular $Ca^{2+}$ Homeostasis in Muscle Tissues

To set the stage for our discussion of MLCKs, it is necessary to understand the intracellular  $Ca^{2+}$  homeostasis in muscle tissues, because  $Ca^{2+}$  is a trigger of MLCK activation and the responses to  $[Ca^{2+}]_i$  differs among the 3 types of muscle cell: smooth muscle, skeletal muscle, and cardiac muscle (Figure 1). Local  $[Ca^{2+}]_i$  transients ( $Ca^{2+}$  sparks), which arise from the coordinated opening of a cluster of ryanodine-sensitive  $Ca^{2+}$  release channels, are necessary for effective  $Ca^{2+}$  signaling in all 3 types of muscle cell, although the rates of  $Ca^{2+}$  transients and contraction vary considerably in the different muscle cells. In general, however, these rates are slower in smooth muscle cells than in either skeletal or cardiac muscle cells. Smooth muscle cells gradually contract according to this slow increase in the level of  $[Ca^{2+}]_i$ .<sup>8</sup> In skeletal muscle cells, the activation of the voltage-gated  $Ca^{2+}$  channel in the transverse tubule mem-

Received May 20, 2013; revised manuscript received June 7, 2013; accepted June 17, 2013; released online July 18, 2013  
Department of Molecular Cardiology, Osaka University Graduate School of Medicine, Suita (O.T.); Department of Cardiovascular Medicine, National Cerebral and Cardiovascular Center, Suita (M.K.), Japan

Mailing address: Osamu Tsukamoto, MD, PhD, Department of Molecular Cardiology, Osaka University Graduate School of Medicine, 2-2 Yamadaoka, Suita 565-0871, Japan. E-mail: tsuka@medone.med.osaka-u.ac.jp

ISSN-1346-9843 doi:10.1253/circj.CJ-13-0627

All rights are reserved to the Japanese Circulation Society. For permissions, please e-mail: [cj@j-circ.or.jp](mailto:cj@j-circ.or.jp)

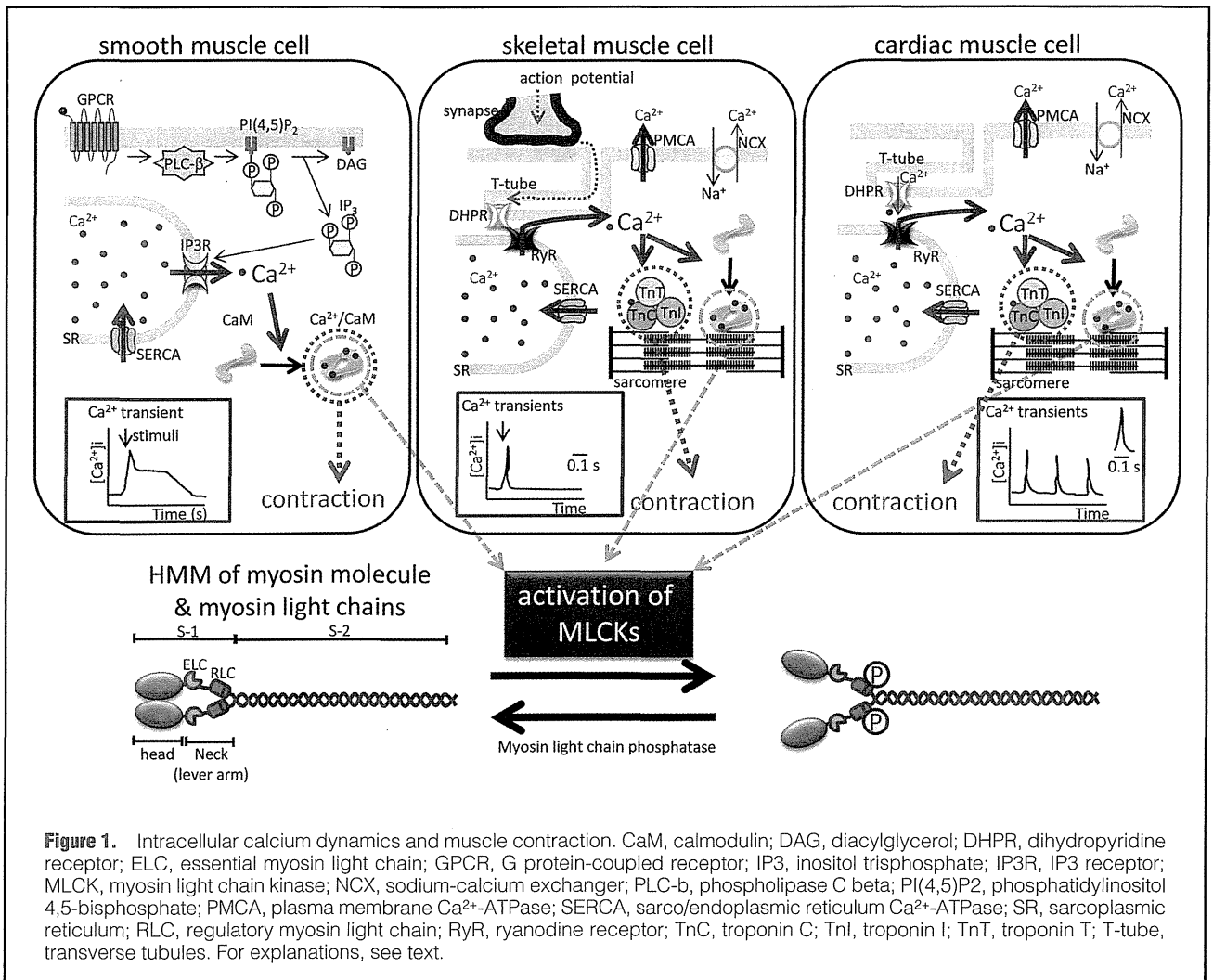


**Figure 1.** Intracellular calcium dynamics and muscle contraction. CaM, calmodulin; DAG, diacylglycerol; DHPR, dihydropyridine receptor; ELC, essential myosin light chain; GPCR, G protein-coupled receptor; IP<sub>3</sub>, inositol trisphosphate; IP<sub>3</sub>R, IP<sub>3</sub> receptor; MLCK, myosin light chain kinase; NCX, sodium-calcium exchanger; PLC-β, phospholipase C beta; PI(4,5)P<sub>2</sub>, phosphatidylinositol 4,5-bisphosphate; PMCA, plasma membrane Ca<sup>2+</sup>-ATPase; SERCA, sarco/endoplasmic reticulum Ca<sup>2+</sup>-ATPase; SR, sarcoplasmic reticulum; RLC, regulatory myosin light chain; RyR, ryanodine receptor; TnC, troponin C; TnI, troponin I; TnT, troponin T; T-tube, transverse tubules. For explanations, see text.

branes directly opens the ryanodine-sensitive Ca<sup>2+</sup> release receptor on the sarcoplasmic reticulum (SR), which results in a rapid increase in [Ca<sup>2+</sup>]<sub>i</sub>. In cardiac muscle cells, electrostimulation from the sinus node activates the voltage-dependent cation channel and thus increases the [Ca<sup>2+</sup>]<sub>i</sub> level, which induces a rapid and large release of Ca<sup>2+</sup> from the SR, known as “Ca<sup>2+</sup>-induced Ca<sup>2+</sup> release”. Importantly, the duration of the increased [Ca<sup>2+</sup>]<sub>i</sub> level in striated muscle cells is very short because the released Ca<sup>2+</sup> is rapidly recaptured in the SR. In cardiac myocytes, electrostimulation increases [Ca<sup>2+</sup>]<sub>i</sub> from 100 nmol/L to a few hundred nmol/L (~1 μmol/L), which returns to the basal level within 0.1 s.

We now attempt to show why striated muscle cells do not use MLCK as a sensor of [Ca<sup>2+</sup>]<sub>i</sub> and an initiator of muscle contraction. The slow kinase reactions of MLCKs are not suitable as a [Ca<sup>2+</sup>]<sub>i</sub> sensor in striated muscles,<sup>4</sup> in which rapid and transient increase in the [Ca<sup>2+</sup>]<sub>i</sub> occurs. Instead, using a non-enzyme signal from the binding of Ca<sup>2+</sup> to troponin, these cells contract promptly in response to the increased [Ca<sup>2+</sup>]<sub>i</sub>. Thus, the increase in [Ca<sup>2+</sup>]<sub>i</sub> during muscle contraction exhibits distinct molecular kinetics in the 3 types of muscle, and these kinetics are related to the different physiological mechanisms that regulate contraction in these muscles.

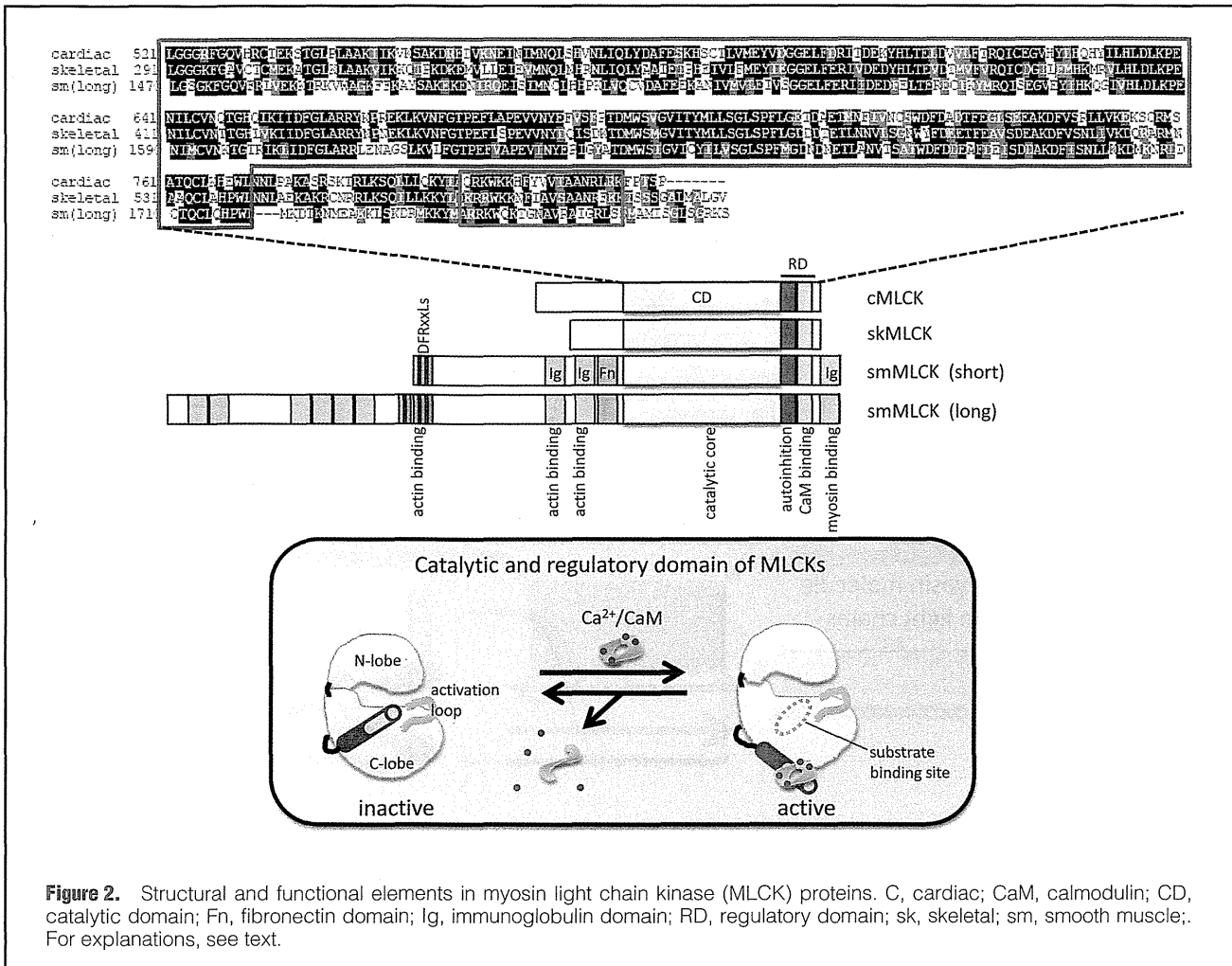
### Mechanism of MLCK Activation by Ca<sup>2+</sup>/Calmodulin Binding

An increase in [Ca<sup>2+</sup>]<sub>i</sub> can enhance MLCK activity approximately 1,000-fold through binding to calmodulin. Ca<sup>2+</sup>/calmodulin is the most important regulator of MLCKs. MLCK is catalytically inactive in the absence of Ca<sup>2+</sup>/calmodulin because the autoinhibitory sequence of MLCK blocks the access of the substrate to the catalytic core (Figure 2).<sup>9</sup> The binding of Ca<sup>2+</sup>/calmodulin to the calmodulin-binding domain displaces the autoinhibitory sequence from the surface of the catalytic core, which results in exposure of the catalytic site of the kinase and thus provides access to the N-terminus of MLC2.<sup>9</sup> MLCK is maximally activated by Ca<sup>2+</sup>/calmodulin at a molar ratio of 1:1 with a dissociation constant of 1 nmol/L.<sup>10</sup>

### Biochemistry of MLCKs

#### smMLCK

smMLCK is encoded by the single-copy MYLK1 gene, which expresses 3 transcripts in a cell-specific manner related to alternative initiation sites: non-muscle isoform (longer form), smooth muscle isoform (shorter form), and telokin.<sup>11</sup> Normally, smooth muscle expresses the shorter form of smMLCK. The smooth muscle isoform contains 3 DFRxxL motifs, a



proline-rich repeat, 3 immunoglobulin (Ig) modules, 1 fibronectin (Fn) module, and 1 kinase domain with a catalytic core and a regulatory segment. The 3 DFRxxL motifs at the N-terminus of smMLCK, which are not present in either of the striated muscle MLCKs, bind to thin actin filaments<sup>10</sup> through an extension of the catalytic core toward the myosin thick filaments for the phosphorylation of the smooth muscle MLC2 at Ser-19 (Figure 2).<sup>12</sup> smMLCK-induced Ser-19 phosphorylation activates myosin ATPase and initiates muscle contraction.<sup>3</sup> Interestingly, different kinases are also known to phosphorylate smMLCK2. Rho-associated coiled-coil forming kinase (ROCK) phosphorylates smMLCK2 at Ser-19 to regulate the assembly of stress fibers.<sup>13</sup> Protein kinase C (PKC) phosphorylates Ser-1/Ser-2/Thr-9, which inhibits myosin ATPase activity.<sup>14</sup> In contrast, several protein kinases, including PKA, PKC, CaMKII, and PAK, are reported to phosphorylate serine residues in the calmodulin-binding sequence in the regulatory domain in vitro, which results in a 10-fold increase in  $K_{cam}$ .<sup>15</sup> On the other hand, the phosphorylation of smMLCK at Thr-40 and Thr-43 by extracellular signal-regulated kinase (ERK) increases  $V_{max}$  without changing  $K_{cam}$ .<sup>15</sup> ATP, which is the other substrate of MLCK, can bind to the MLCK catalytic core regardless of the positioning of the autoinhibitory sequence.<sup>12</sup>  $K_m$  for ATP is approximately 50–150  $\mu\text{mol/L}$ .<sup>12</sup> The concentrations of smMLCK and its substrate, smMLCK2, are approximately 4  $\mu\text{mol/L}$  and 30–40  $\mu\text{mol/L}$ , respectively.<sup>8</sup>

### skMLCK

skMLCK is encoded by the MYLK2 gene and is predominantly expressed in skeletal muscle, although it was originally cloned from cardiac muscle.<sup>16</sup> skMLCK is reported to weakly bind to myofilaments,<sup>10</sup> likely because it lacks the actin binding domain that is found in smMLCK (Figure 2). skMLCK phosphorylates skeletal muscle MLC2 (skMLCK2) at Ser-15.<sup>17</sup> In contrast to smMLCK, which phosphorylates only smooth muscle MLC2 efficiently, skMLCK can phosphorylate other MLC2s found in cardiac and smooth muscles that exhibit similar catalytic properties.<sup>17</sup> Previous physiological studies have demonstrated that the extent of MLC2 phosphorylation in skeletal muscle increases from 0–10% to 40–60% depending on the frequency of muscle stimulation.<sup>17</sup>

### cMLCK

cMLCK is encoded by the MYLK3 gene and expressed exclusively in the heart, both the atria and ventricles.<sup>18</sup> cMLCK is structurally related to both skMLCK and smMLCK and contains a conserved kinase domain at its C-terminus that exhibits 58% identity with skMLCK and 44% identity with smMLCK.<sup>7,18</sup> However, the N-terminus of cMLCK lacks homologies to known proteins, including other MLCKs, which indicates that cMLCK may play some specific functional roles (Figure 2). Immunostaining of endogenous cMLCK in cardiac myocytes has shown a diffuse positive staining pattern in

Table. Biochemical Characteristics of Protein Kinases in the Heart						
Kinase	Gene	Substrate	$K_m$ ( $\mu\text{mol/L}$ )	$V_{max}$ ( $\mu\text{mol} \cdot \text{min}^{-1} \cdot \text{mg}^{-1}$ )	$V_{max}/K_m$	
Cardiac MLCK	MYLK3	MLC2v	$4.3 \pm 1.5$	$0.26 \pm 0.06$	0.06	
Skeletal MLCK	MYLK2	Skeletal MLC2	$4.3 \pm 0.5$	$40 \pm 1.7$	9.3	
Smooth muscle MLCK	MYLK1	Smooth muscle MLC2	$8.3 \pm 1.4$	$28 \pm 5.8$	3.5	
ZIPK	DAPK3	MLC2v	$15.2 \pm 2.0$	$0.89 \pm 0.05$	0.06	
		Smooth muscle MLC2	$1.8 \pm 0.3$	$0.42 \pm 0.03$	0.23	

MLCK, myosin light chain kinase; MLC2v, ventricular myosin regulatory chain-2; ZIPK, zipper-interacting protein kinase.

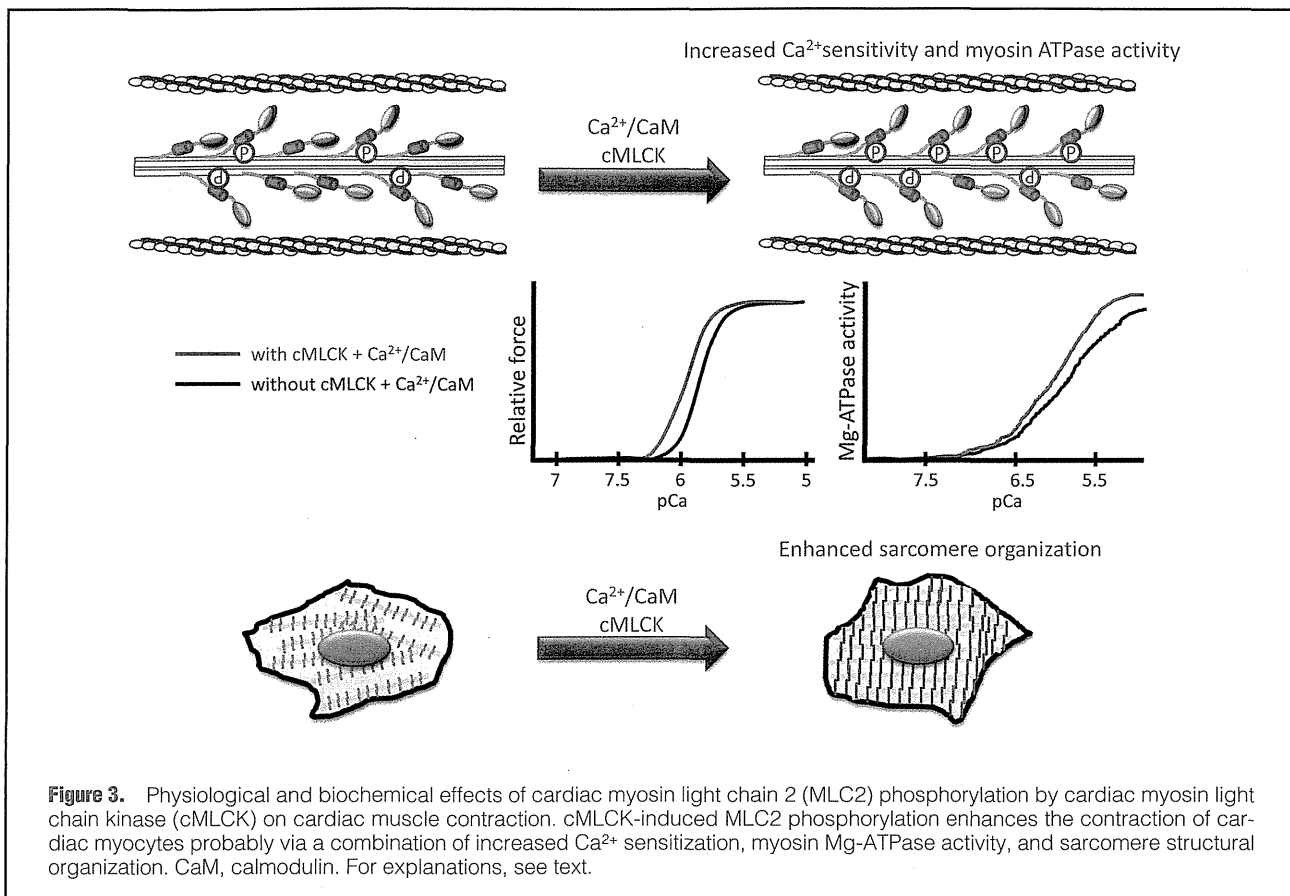


**Figure 3.** Physiological and biochemical effects of cardiac myosin light chain 2 (MLC2) phosphorylation by cardiac myosin light chain kinase (cMLCK) on cardiac muscle contraction. cMLCK-induced MLC2 phosphorylation enhances the contraction of cardiac myocytes probably via a combination of increased  $\text{Ca}^{2+}$  sensitization, myosin Mg-ATPase activity, and sarcomere structural organization. CaM, calmodulin. For explanations, see text.

the cytoplasm with a striated staining pattern in the cell periphery.<sup>18</sup> Interestingly, the striated MLCK staining colocalized with actin but not with its substrate.<sup>18</sup> Chan et al reported the independence of cMLCK activity from  $\text{Ca}^{2+}$ /calmodulin,<sup>18</sup> which was an unexpected result, because cMLCK also contains both autoinhibitory and calmodulin-binding sequences, similar to the other 2 types of MLCKs, and binds to calmodulin with high affinity in a  $\text{Ca}^{2+}$ -dependent manner.<sup>7,19</sup> There are conflicting results concerning the  $\text{Ca}^{2+}$ /calmodulin dependency of cMLCK activity,<sup>7,19</sup> and thus requires further examination.

The Table demonstrates the estimated kinetic constants of each MLCK determined by Lineweaver-Burk plots.<sup>18,20-22</sup> cMLCK has a high affinity for its substrate, similar to skMLCK and smMLCK. However, the catalytic efficiency of cMLCK, which is indicated by the  $V_{max}/K_m$  ratio, is lower than that of skMLCK and smMLCK. Thus, the maximal specific kinase activity of cMLCK is much lower than that of sm-

MLCK and skMLCK. However, the low specific activity of cMLCK results in a slow turnover of phosphate in MLC2 ( $t_{1/2}=250$  min), with an MLC2 basal phosphorylation of approximately 0.2–0.4 mol of phosphate/mol of MLC2 under basal conditions,<sup>23-26</sup> which indicates that the kinase activity of cMLCK may be a primary limiting factor of MLC2 phosphorylation.<sup>19</sup>

### Structural Changes of Myosin Head Induced by MLC2 Phosphorylation in Striated Muscles

Muscle myosin is the molecular motor in the thick filament of the sarcomere and is composed of 1 pair of myosin heavy chains (MHC) and 2 pairs of myosin light chains (MLC): essential MLC and regulatory MLC (ie, MLC2) (Figure 1). Both of the MLCs wrap around the neck region of the MHC. MLC2 is positioned at the S1–S2 junction of the MHC through its binding to a 35-amino-acid IQ motif on the MHC.<sup>27</sup> The MLC2

contains a highly conserved serine that is phosphorylatable by MLCK and plays an important role in the activation and modulation of myosin by fine-tuning the motion of the neck region of the MHC.<sup>10</sup> The MLC2 also contains a  $\text{Ca}^{2+}/\text{Mg}^{2+}$  binding site at its N-terminus from Asp-37 to Asp-48, located in the first helix-loop-helix motif, and the binding of divalent cation alters the structural and contractile properties.<sup>28,29</sup> The neck region of the myosin head has been proposed to act as a lever arm. The phosphorylation of MLC2 at Ser-15 results in the addition of a negative charge to the N-terminal region of MLC2, which induces the myosin head to swing out from a position close to the thick filament's backbone toward the actin filament, and this structural change increases the rate through which the myosin-actin interaction occurs and promotes force generation at a given level of  $\text{Ca}^{2+}$  (Figures 1,3).<sup>30,31</sup> Interestingly, several mutations around the phosphorylatable Ser-15 and the  $\text{Ca}^{2+}$  binding site in MLC2 have been found in patients with familial hypertrophic cardiomyopathy.<sup>32-34</sup>

### PKs and Protein Phosphatase Regulation of MLC2 Phosphorylation in the Heart

There are 2 types of cardiac MLC2: a ventricular myosin light chain-2 (MLC2v) and an atrium-specific form (MLC2a).<sup>35</sup> All 3 MLCKs are expressed in the heart. However, the amount of skMLCK in the heart is too low to maintain cardiac MLC2 phosphorylation,<sup>36</sup> and ablation of skMLCK has no effect on MLC2 phosphorylation in cardiac muscle,<sup>36</sup> which indicates that skMLCK does not play a major role in MLC2v phosphorylation. The expression of smMLCK in the heart is also 10- to 20-fold lower than that of cMLCK,<sup>18</sup> and cardiac MLC2 is not a good substrate for smMLCK.<sup>36</sup> smMLCK may phosphorylate non-muscle cytoplasmic myosin II-B and plays an important role in the heart.<sup>37</sup> Thus, there are currently 2 candidate kinases for MLC2 phosphorylation in cardiac myocytes: cMLCK<sup>7,18</sup> and zipper-interacting PK (ZIPK).<sup>38</sup> ZIPK is a  $\text{Ca}^{2+}$ -independent serine/threonine kinase that has been implicated in apoptosis and is ubiquitously expressed, including in adult and neonatal cardiac myocytes.<sup>39</sup> In permeabilized smooth muscle cells, constitutively active ZIPK initiates contraction through the phosphorylation of smooth muscle MLC2.<sup>40</sup> Cardiac MLC2 was also identified as a biochemically favorable substrate for ZIPK through an unbiased substrate search with purified ZIPK on heart homogenates and was phosphorylated at Ser-15 in vivo and in vitro by ZIPK.<sup>38</sup> In fact,  $V_{\text{max}}$  for cardiac MLC2 is 2-fold greater than that obtained for smooth muscle MLC2 ( $887 \pm 47$  and  $415 \pm 49 \text{ nmol} \cdot \text{min}^{-1} \cdot \text{mg}^{-1}$ , respectively), whereas the  $K_m$  of cardiac MLC2 is higher than that of smooth muscle MLC2 ( $15.0 \pm 2.0$  and  $1.8 \pm 0.3 \mu\text{mol/L}$ , respectively).<sup>38</sup> However, ZIPK is considered not to be involved in the basal phosphorylation of cardiac MLC2 in vivo,<sup>41</sup> although knockdown of ZIPK in cardiac myocytes by siRNA decreased the extent of cardiac regulatory MLC phosphorylation by 34%.<sup>38</sup> The physiological role of ZIPK-induced cardiac MLC2 phosphorylation remains unknown.

It is now well established that cMLCK is the predominant cardiac MLC2 kinase responsible for basal phosphorylation in vivo, because the ablation of cMLCK almost completely abolishes the phosphorylation of MLC2v.<sup>7,18,25,41</sup> Ding et al demonstrated that a partial reduction in the amount of cMLCK protein in cMLCK hetero knockout mice (cMLCK<sup>+neo</sup>) resulted in a partial reduction in MLC2 phosphorylation in both ventricular and atrial muscles, and this reduction in MLC2 phosphorylation was proportional to the cMLCK expression level.<sup>41</sup> In addition, the overexpression of cMLCK increases MLC2v

phosphorylation in a dose-dependent manner and, conversely, knockdown of cMLCK by RNAi decreases MLC2v phosphorylation in vitro.<sup>18</sup> Scruggs et al identified 3 distinct charge variants of endogenous MLC2v in vivo in the mouse: unphosphorylated, singly phosphorylated, and doubly phosphorylated at Ser-14/Ser-15.<sup>42</sup> In contrast, Ser-14 in murine MLC2v is replaced by Asn in human MLC2. However, human MLC2 also has 3 distinct charge variants in vivo: unphosphorylated, singly phosphorylated at Ser-15, and deamidated Asn-14/phosphorylated Ser-15.<sup>42</sup> Interestingly, the deamination of Asn to Asp can create a negative charge similar to that obtained through phosphorylation.<sup>26</sup> In addition, there is a spatial gradient of MLC2v phosphorylation through the ventricular wall: relatively low in the inner layer and high in the outer layer.<sup>16,43</sup> This gradient, which may be caused by reduced activity of the phosphatase in the outer layer,<sup>44,45</sup> may be important for normalizing wall stress and contributes to efficient contraction of the whole heart.<sup>16</sup>

The level of MLC2v phosphorylation is maintained relatively constant by the appropriate balance between phosphorylation by cMLCK and dephosphorylation by phosphatase in the physiologically constant beating heart. The dephosphorylation of MLC2v is mediated mainly by catalytic subunit of type 1 phosphatase (PP1c- $\delta$ ) in concert with myosin phosphatase target subunit 2 (MYPT2).<sup>46</sup> In contrast, MLC2 phosphorylation by MLCK is transient in both smooth and skeletal muscle cells, although they have different MLC2 phosphorylation dynamics.<sup>19</sup> MLC2 phosphorylation is rapidly dephosphorylated by robust myosin light chain phosphatase activity in smooth muscle cells, whereas MLC2 phosphorylation is prolonged and slowly dephosphorylated by the low myosin light chain phosphatase activity in skeletal muscle cells.

### Physiological Regulators of cMLCK Expression and Activity

The expression of cMLCK is highly regulated by the cardiac homeobox protein Nkx2-5 in neonatal cardiac myocytes.<sup>18</sup> cMLCK mRNA increases during development to adult stages and persists in the aged heart, whereas its protein level decreases in the aged heart, which suggests an alternation in post-transcriptional regulation.<sup>18</sup> Exercise has been reported to increase cMLCK expression and MLC2v phosphorylation.<sup>25</sup> Catalytic activity may be regulated by phosphorylation through upstream kinases.<sup>47</sup> cMLCK has several potential phosphorylation sites for other kinases, such as PKA and PKC,<sup>18</sup> although more studies are required to clarify the details of this mechanism.

Hypertrophic agonists, such as  $\alpha 1$ - or  $\beta 1$ -adrenergic stimulation<sup>18,48,49</sup> and angiotensin II, induce MLC2v phosphorylation through MLCK activation in both cultured cardiac myocytes and the adult heart in vivo.<sup>24</sup> Other neurohumoral stimulators, such as endothelin<sup>50</sup> and prostanoid F receptors,<sup>51</sup> have also been reported to increase MLC2 phosphorylation and induce a prominent increase in the contractile force in the heart. Neuregulin, which activates ErbB receptor tyrosine kinase, has been reported to enhance the expression of cMLCK with a concomitant increase in MLC2v phosphorylation and improved cardiac performance after myocardial infarction in rats.<sup>52</sup>

### Role of MLC2 Phosphorylation in Sarcomere Organization and Heart Development

The transfection of cardiac myocytes with skMLCK has resulted in the phosphorylation of MLC2v and led to a highly

organized sarcomeric pattern without induction of other hypertrophic phenotypes, such as the induction of fetal genes and an increase in cell size.<sup>24</sup> Furthermore, the dominant-negative kinase-inactive form of MLCK completely prevents sarcomere organization in response to angiotensin II,<sup>24</sup> which suggests that MLCK activation is necessary and sufficient to induce sarcomere organization (Figure 3). Consistent with these findings, the adenovirus-mediated overexpression of cMLCK in cardiac myocytes promotes sarcomere organization characterized by straight, thick, striated actin bundles,<sup>48</sup> whereas re-establishment of the phenylephrine-induced sarcomere structure is inhibited by pretreatment with RNAi against cMLCK.<sup>7</sup> Interestingly, the reduced cMLCK expression induced by the antisense morpholino causes severely impaired heart development in zebrafish and histological analysis showed that the structure of the sarcomere was poorly developed compared with control zebrafish.<sup>7</sup> However, studies with transgenic and knockout mice have shown that MLC2v phosphorylation is not critical for cardiogenesis in the mammalian system,<sup>18,41,53</sup> although it is necessary for the optimal contractile performance of the heart.

### Physiological Role of MLC2 Phosphorylation in the Heart

The degree of MLC2 phosphorylation is known to play a critical role in the determination of the Ca<sup>2+</sup>-sensitive cross-bridge transition in skeletal muscle.<sup>54</sup> In permeable cardiac muscle fibers, MLC2 phosphorylation induced by MLCK increases the Ca<sup>2+</sup> sensitivity, which manifests as a leftward shift in the force-Ca<sup>2+</sup> relationship, and MLC2 dephosphorylation by phosphatase decreases the Ca<sup>2+</sup> sensitivity (ie, dephosphorylation resulted in Ca<sup>2+</sup> desensitization).<sup>55,56</sup> MLC2 phosphorylation by MLCK is also associated with enhanced Ca<sup>2+</sup>-stimulated myosin Mg-ATPase activity in rat cardiac myofibrils (Figure 3).<sup>57</sup> In the rat heart, MLC2v phosphorylation increases in response to an increase in the beat frequency and/or left ventricular pressure by exercise or inotropic agents, which may help augment the peak left ventricular pressure.<sup>58,59</sup> At the cellular level, adenovirus-mediated overexpression of cMLCK potentiates the amplitude of the contraction of cardiac myocytes and the kinetics of contraction and relaxation without changing the [Ca<sup>2+</sup>]<sub>i</sub> transients.<sup>18</sup>

Several studies have also addressed the role of MLC2 phosphorylation in the heart using genetically modified mice. Huang et al<sup>60</sup> generated transgenic mice expressing skMLCK specifically in cardiac myocytes (TG-skMLCK). These TG-skMLCK mice demonstrated marked increases in the phosphorylation of both cardiac MLC2 and cytoplasmic non-muscle MLC2 in the heart without significant cardiac hypertrophy or structural abnormalities up to 6 months of age, which indicates that increased cardiac MLC2 phosphorylation per se does not cause cardiac hypertrophy.<sup>60</sup> Interestingly, the hypertrophic cardiac response to exercise and isoproterenol treatment was attenuated in TG-skMLCK mice,<sup>26</sup> which supports the hypothesis that the phosphorylation of cardiac MLC2 may inhibit physiological and pathophysiological hypertrophic responses through enhanced contractile performance and efficiency. Sanbe et al<sup>53</sup> created transgenic mice (TG-MLC2v(P-)) in which 3 potentially phosphorylatable serines (Ser-14/Ser-15/Ser-19) in the MLC2v (ventricular regulatory myosin light chain) were mutated to alanine. After MLCK treatment, the isolated ventricular fibers from the non-transgenic control mice showed increased Mg-ATPase activity and Ca<sup>2+</sup> sensitivity, as indicated by a leftward shift in the force-Ca<sup>2+</sup> curve,

whereas the fibers from the TG-MLC2v(P-) mice did not exhibit these increases.<sup>53</sup> This suppressed performance of muscle fibers with nonphosphorable MLC2v is consistent with the demonstrated effects of MLC2 phosphorylation in skeletal muscle.<sup>36</sup> Scruggs et al<sup>48</sup> examined the role of regulatory myosin light chain 2 phosphorylation in the ejection of the hearts of TG-MLC2v(P-) mice by measuring the systolic mechanics under basal conditions and in response to adrenergic stimulation. The TG-MLC2v(P-) mice demonstrated depressed contractility, decreased maximal left ventricular power development, and a decrease in the time-to-peak elastance during ejection under basal conditions.<sup>48</sup> Interestingly, the TG-MLC2v(P-) mice exhibited a blunting of the positive inotropic response to  $\beta$ 1-adrenergic stimulation.<sup>48</sup> Because cMLCK has multiple PKA consensus sequences in its unique N-terminus region,<sup>26</sup> and  $\beta$ 1-adrenergic stimulation increased MLC2v Ser-15 phosphorylation in hearts of non-transgenic control mice<sup>48</sup>, there might be a possible relationship between  $\beta$ 1-adrenergic signaling and MLC2v phosphorylation. The TG-MLC2v(P-) mice developed cardiac hypertrophy at 3–4 months of age, most likely because of a compensatory hypertrophic growth response to diminished contractile performance.<sup>53</sup> cMLCK-knockout mice (cMLCK<sup>neo/neo</sup>) also demonstrated the critical role of cMLCK in normal physiological cardiac function, with decreased cardiac performance and the induction of cardiac hypertrophy at 4–5 months of age.<sup>41</sup> In contrast, transgenic mice overexpressing MYPT2 specifically in cardiac myocytes demonstrated enhanced expression of MYPT2 with a concomitant increase in the level of endogenous PP1c- $\delta$ , which resulted in a reduction of the level of in vivo MLC2v phosphorylation in the heart associated with a decrease in the myofilament response to Ca<sup>2+</sup> and a decreased left ventricular contractility.<sup>61</sup> These findings are consistent with the evidence obtained from TG-MLC2v(P-) mice and cMLCK-knockout mice as mentioned earlier.

Surprisingly, Warren et al recently reported an inverse relationship between cMLCK expression and systolic pressure: cMLCK expression is higher in the right ventricular myocardium than the left ventricular myocardium.<sup>25</sup> Because the cMLCK expression in the left ventricle was markedly downregulated as a result of pressure overload, those authors speculated that increased mechanical stress reduces the net expression of cMLCK.<sup>25</sup>

### cMLCK in Heart Diseases

cMLCK was first identified through the integrated cDNA expression analysis of failing human myocardium, which showed that the cMLCK mRNA expression levels correlated well with the pulmonary arterial pressure of patients with heart failure.<sup>7</sup> Decreased phosphorylation of MLC2 was also reported in some patients with heart failure.<sup>62,63</sup> In animal models of myocardial infarction, the expression level of cMLCK in the heart has been found to be reduced.<sup>18,52</sup> In addition, pressure overload also led to a marked reduction in cMLCK and phosphorylated MLC2v in the heart 1 week after thoracic aortic constriction surgery.<sup>25</sup> Interestingly, the reduction in the cMLCK protein level in pressure-overloaded hearts was mediated by upregulation of the ubiquitin-proteasome degradation system.<sup>25</sup> The specific overexpression of cMLCK in cardiac myocytes attenuated the phenotype of the pressure overload-induced heart failure,<sup>25</sup> and this finding suggests a protective role of cMLCK against cardiac stress.

Induced pluripotent stem cell-derived cardiac myocytes (iPSC-CMs) are expected to become a new cell therapy for

heart diseases and iPSC-CMs express cardiac-specific proteins similar to neonatal cardiac myocytes.<sup>64</sup> However, so far there are no reports of investigations into cMLCK and MLC2 phosphorylation in iPSC-CMs.

### New Approach to Finding Potential Inhibitors or Activators of Kinases

Recently, Suga et al developed a new technology to discover “natural product-like” nonstandard peptides against various therapeutic targets, and this technology, which is known as the RaPID (Random non-strand Peptides Integrated Discovery) system, comprises a FIT (Flexible in vivo Translation) system coupled with an mRNA display.<sup>65</sup> Using this system, Suga et al successfully isolated anti-E6AP macrocyclic *N*-methyl-peptides, one of which had high affinity ( $K_a=0.60$  nmol/L) against a target E6AP and strongly suppressed its polyubiquitination ability against p53.<sup>66</sup> Because the targets of the RaPID system are not limited, this technology can be applied to the discovery of kinase activators or inhibitors.

### Conclusion

We are now attempting to find a new potential activator or inhibitor of cMLCK, which will hopefully either provide new insights to cMLCK or be successfully applied in the clinical setting.

### Acknowledgments

This research was supported by the Japan Society for the Promotion of Science (JSPS) through the “Funding Program for Next Generation World-Leading Researchers (NEXT Program),” initiated by the Council for Science and Technology Policy (CSTP); grants-in-aid from the Ministry of Health, Labor, and Welfare-Japan; grants-in-aid from the Ministry of Education, Culture, Sports, Science, and Technology-Japan. The research was also supported by grants from the Japan Heart Foundation, Japan Cardiovascular Research Foundation, Japan Cardiovascular Research Foundation, Japan Foundation of Applied Enzymology.

Conflict of Interest: The authors have no conflicts of interest to declare.

### References

- Huxley H, Hanson J. Changes in the cross-striations of muscle during contraction and stretch and their structural interpretation. *Nature* 1954; **171**: 370–378.
- Ebashi F, Ebashi S. Removal of calcium and relaxation in actomyosin systems. *Nature* 1962; **194**: 378–379.
- Kamm KE, Stull JT. The function of myosin and myosin light chain kinase phosphorylation in smooth muscle. *Annu Rev Pharmacol Toxicol* 1985; **25**: 593–620.
- Koizumi K, Hoshiai M, Ishida H, Ohyama K, Sugiyama H, Naito A, et al. Stanniocalcin 1 prevents cytosolic  $Ca^{2+}$  overload and cell hypercontracture in cardiomyocytes. *Circ J* 2007; **71**: 796–801.
- Ebashi S, Kodama A. A new protein factor promoting aggregation of tropomyosin. *J Biochem* 1965; **58**: 107–108.
- Kajioka S, Takahashi-Yanaga F, Shahab N, Onimaru M, Matsuda M, Takahashi R, et al. Endogenous cardiac troponin T modulates  $Ca^{2+}$ -mediated smooth muscle contraction. *Sci Rep* 2012; **2**: 979.
- Seguchi O, Takashima S, Yamazaki S, Asakura M, Asano Y, Shintani Y, et al. A cardiac myosin light chain kinase regulates sarcomere assembly in the vertebrate heart. *J Clin Invest* 2007; **117**: 2812–2824.
- Takashima S. Phosphorylation of myosin regulatory light chain by myosin light chain kinase, and muscle contraction. *Circ J* 2009; **73**: 208–213.
- Chin D, Means AR. Calmodulin: A prototypical calcium sensor. *Trends Cell Biol* 2000; **10**: 322–328.
- Sweeney HL, Bowman BF, Stull JT. Myosin light chain phosphorylation in vertebrate striated muscle: Regulation and function. *Am J Physiol* 1993; **264**: C1085–C1095.
- Birukov KG, Schavocky JP, Shirinsky VP, Chibalina MV, Van Eldik LJ, Watterson DM. Organization of the genetic locus for chicken myosin light chain kinase is complex: Multiple proteins are encoded and exhibit differential expression and localization. *J Cell Biochem* 1998; **70**: 402–413.
- Hong F, Haldeman BD, Jackson D, Carter M, Baker JE, Cremona CR. Biochemistry of smooth muscle myosin light chain kinase. *Arch Biochem Biophys* 2011; **510**: 135–146.
- Totsukawa G, Yamakita Y, Yamashiro S, Hartshorne DJ, Sasaki Y, Matsumura F. Distinct roles of ROCK (Rho-kinase) and MLCK in spatial regulation of MLC phosphorylation for assembly of stress fibers and focal adhesions in 3T3 fibroblasts. *J Cell Biol* 2000; **150**: 797–806.
- Ikebe M, Hartshorne DJ, Elzinga M. Phosphorylation of the 20,000-dalton light chain of smooth muscle myosin by the calcium-activated, phospholipid-dependent protein kinase: Phosphorylation sites and effects of phosphorylation. *J Biol Chem* 1987; **262**: 9569–9573.
- Kamm KE, Stull JT. Dedicated myosin light chain kinases with diverse cellular functions. *J Biol Chem* 2001; **276**: 4527–4530.
- Davis JS, Hassanzadeh S, Winitzky S, Lin H, Satorius C, Vemuri R, et al. The overall pattern of cardiac contraction depends on a spatial gradient of myosin regulatory light chain phosphorylation. *Cell* 2001; **107**: 631–641.
- Stull JT, Kamm KE, Vandenberg R. Myosin light chain kinase and the role of myosin light chain phosphorylation in skeletal muscle. *Arch Biochem Biophys* 2011; **510**: 120–128.
- Chan JY, Takeda M, Briggs LE, Graham ML, Lu JT, Horikoshi N, et al. Identification of cardiac-specific myosin light chain kinase. *Circ Res* 2008; **102**: 571–580.
- Kamm KE, Stull JT. Signaling to myosin regulatory light chain in sarcomeres. *J Biol Chem* 2011; **286**: 9941–9947.
- Zhi G, Herring BP, Stull JT. Structural requirements for phosphorylation of myosin regulatory light chain from smooth muscle. *J Biol Chem* 1994; **269**: 24723–24727.
- Herring BP, Gallagher PJ, Stull JT. Substrate specificity of myosin light chain kinases. *J Biol Chem* 1992; **267**: 25945–25950.
- Ikebe M, Reardon S, Schwonek JP, Sanders CR 2nd, Ikebe R. Structural requirement of the regulatory light chain of smooth muscle myosin as a substrate for myosin light chain kinase. *J Biol Chem* 1994; **269**: 28165–28172.
- Herring BP, England PJ. The turnover of phosphate bound to myosin light chain-2 in perfused rat heart. *Biochem J* 1986; **240**: 205–214.
- Aoki H, Sadoshima J, Izumo S. Myosin light chain kinase mediates sarcomere organization during cardiac hypertrophy in vitro. *Nat Med* 2000; **6**: 183–188.
- Warren SA, Briggs LE, Zeng H, Chuang J, Chang EI, Terada R, et al. Myosin light chain phosphorylation is critical for adaptation to cardiac stress. *Circulation* 2012; **126**: 2575–2588.
- Scruggs SB, Solaro RJ. The significance of regulatory light chain phosphorylation in cardiac physiology. *Arch Biochem Biophys* 2011; **510**: 129–134.
- Rayment I, Rypniewski WR, Schmidt-Base K, Smith R, Tomchick DR, Benning MM, et al. Three-dimensional structure of myosin subfragment-1: A molecular motor. *Science* 1993; **261**: 50–58.
- Reinach FC, Nagai K, Kendrick-Jones J. Site-directed mutagenesis of the regulatory light-chain  $Ca^{2+}/Mg^{2+}$  binding site and its role in hybrid myosins. *Nature* 1986; **322**: 80–83.
- Szczesna-Cordary D, Guzman G, Ng SS, Zhao J. Familial hypertrophic cardiomyopathy-linked alterations in  $Ca^{2+}$  binding of human cardiac myosin regulatory light chain affect cardiac muscle contraction. *J Biol Chem* 2004; **279**: 3535–3542.
- Levine RJ, Chantler PD, Kensler RW, Woodhead JL. Effects of phosphorylation by myosin light chain kinase on the structure of Limulus thick filaments. *J Cell Biol* 1991; **113**: 563–572.
- Levine RJ, Kensler RW, Yang Z, Stull JT, Sweeney HL. Myosin light chain phosphorylation affects the structure of rabbit skeletal muscle thick filaments. *Biophys J* 1996; **71**: 898–907.
- Szczesna D, Ghosh D, Li Q, Gomes AV, Guzman G, Arana C, et al. Familial hypertrophic cardiomyopathy mutations in the regulatory light chains of myosin affect their structure,  $Ca^{2+}$  binding, and phosphorylation. *J Biol Chem* 2001; **276**: 7086–7092.
- Otsuka H, Arimura T, Abe T, Kaiwai H, Aizawa Y, Kubo T, et al. Prevalence and distribution of sarcomeric gene mutations in Japanese patients with familial hypertrophic cardiomyopathy. *Circ J* 2012; **76**: 453–461.
- Niwano S. Multicenter study of the prevalence and distribution of sarcomeric gene mutations in familial hypertrophic cardiomyopathy: A milestone for genetic diagnosis in the Japanese population. *Circ J* 2012; **76**: 303–304.
- Collins JH. Myoinformatics report: Myosin regulatory light chain paralogs in the human genome. *J Muscle Res Cell Motil* 2006; **27**: 69–74.
- Zhi G, Ryder JW, Huang J, Ding P, Chen Y, Zhao Y, et al. Myosin light chain kinase and myosin phosphorylation effect frequency-dependent potentiation of skeletal muscle contraction. *Proc Natl*



- Acad Sci USA* 2005; **102**: 17519–17524.
37. Ma X, Takeda K, Singh A, Yu ZX, Zervas P, Blount A, et al. Conditional ablation of nonmuscle myosin II-B delineates heart defects in adult mice. *Circ Res* 2009; **105**: 1102–1109.
  38. Chang AN, Chen G, Gerard RD, Kamm KE, Stull JT. Cardiac myosin is a substrate for zipper-interacting protein kinase (ZIPK). *J Biol Chem* 2010; **285**: 5122–5126.
  39. Haystead TA. ZIP kinase, a key regulator of myosin protein phosphatase 1. *Cell Signal* 2005; **17**: 1313–1322.
  40. Ihara E, MacDonald JA. The regulation of smooth muscle contractility by zipper-interacting protein kinase. *Can J Physiol Pharmacol* 2007; **85**: 79–87.
  41. Ding P, Huang J, Battiprolu PK, Hill JA, Kamm KE, Stull JT. Cardiac myosin light chain kinase is necessary for myosin regulatory light chain phosphorylation and cardiac performance in vivo. *J Biol Chem* 2010; **285**: 40819–40829.
  42. Scruggs SB, Reisdorph R, Armstrong ML, Warren CM, Reisdorph N, Solaro RJ, et al. A novel, in-solution separation of endogenous cardiac sarcomeric proteins and identification of distinct charged variants of regulatory light chain. *Mol Cell Proteomics* 2010; **9**: 1804–1818.
  43. Hidalgo C, Wu Y, Peng J, Siems WF, Campbell KB, Granzier H. Effect of diastolic pressure on MLC2v phosphorylation in the rat left ventricle. *Arch Biochem Biophys* 2006; **456**: 216–223.
  44. Rajashree R, Blunt BC, Hofmann PA. Modulation of myosin phosphatase targeting subunit and protein phosphatase 1 in the heart. *Am J Physiol Heart Circ Physiol* 2005; **289**: H1736–H1743.
  45. Cohen PT. Protein phosphatase 1: Targeted in many directions. *J Cell Sci* 2002; **115**: 241–256.
  46. Fujioka M, Takahashi N, Odoi H, Araki S, Ichikawa K, Feng J, et al. A new isoform of human myosin phosphatase targeting/regulatory subunit (MYPT2): cDNA cloning, tissue expression, and chromosomal mapping. *Genomics* 1998; **49**: 59–68.
  47. Soderling TR, Stull JT. Structure and regulation of calcium/calmodulin-dependent protein kinases. *Chem Rev* 2001; **101**: 2341–2352.
  48. Scruggs SB, Hinken AC, Thawornkaiwong A, Robbins J, Walker LA, de Tombe PP, et al. Ablation of ventricular myosin regulatory light chain phosphorylation in mice causes cardiac dysfunction in situ and affects neighboring myofilament protein phosphorylation. *J Biol Chem* 2009; **284**: 5097–5106.
  49. Grimm M, Haas P, Willipinski-Stapelfeldt B, Zimmerman WH, Rau T, Pantel K, et al. Key role of myosin light chain (MLC) kinase-mediated MLC2a phosphorylation in the alpha 1-adrenergic positive inotropic effect in human atrium. *Cardiovasc Res* 2005; **65**: 211–220.
  50. Rossmann GH, Hoh JF, Turnbull L, Ludowyke RI. Mechanism of action of endothelin in rat cardiac muscle: Cross-bridge kinetics and myosin light chain phosphorylation. *J Physiol* 1997; **505**: 217–227.
  51. Riise J, Nguyen CH, Qvigstad E, Sandnes DL, Osnes JB, Skomedal T, et al. Prostanoid F receptors elicit an inotropic effect in rat left ventricle by enhancing myosin light chain phosphorylation. *Cardiovasc Res* 2008; **80**: 407–415.
  52. Gu X, Liu X, Xu D, Li X, Yan M, Qi Y, et al. Cardiac functional improvement in rats with myocardial infarction by up-regulating cardiac myosin light chain kinase with neuregulin. *Cardiovasc Res* 2010; **88**: 334–343.
  53. Sanbe A, Fewell JG, Gulick J, Osinska H, Lorenz J, Hall DG, et al. Abnormal cardiac structure and function in mice expressing non-phosphorylatable cardiac regulatory myosin light chain 2. *J Biol Chem* 1999; **274**: 21085–21094.
  54. Patel JR, Diffeo GM, Moss RL. Myosin regulatory light chain modulates the Ca<sup>2+</sup> dependence of the kinetics of tension development in skeletal muscle fibers. *Biophys J* 1996; **70**: 2333–2340.
  55. Morano I, Hofmann F, Zimmer M, Ruegg JC. The influence of P-light chain phosphorylation by myosin light chain kinase on the calcium sensitivity of chemically skinned heart fibres. *FEBS Lett* 1985; **189**: 221–224.
  56. Sweeney HL, Stull JT. Phosphorylation of myosin in permeabilized mammalian cardiac and skeletal muscle cells. *Am J Physiol* 1986; **250**: C657–C660.
  57. Noland TA Jr, Kuo JF. Phosphorylation of cardiac myosin light chain 2 by protein kinase C and myosin light chain kinase increases Ca(2+)-stimulated actomyosin MgATPase activity. *Biochem Biophys Res Commun* 1993; **193**: 254–260.
  58. Fitzsimons DP, Bodell PW, Baldwin KM. Phosphorylation of rodent cardiac myosin light chain 2: Effects of exercise. *J Appl Physiol* 1989; **67**: 2447–2453.
  59. Fitzsimons DP, Bodell PW, Baldwin KM. Myocardial functional correlates of cardiac myosin light chain 2 phosphorylation. *J Appl Physiol* 1990; **68**: 2426–2433.
  60. Huang J, Shelton JM, Richardson JA, Kamm KE, Stull JT. Myosin regulatory light chain phosphorylation attenuates cardiac hypertrophy. *J Biol Chem* 2008; **283**: 19748–19756.
  61. Mizutani H, Okamoto R, Moriki N, Konishi K, Taniguchi M, Fujita S, et al. Overexpression of myosin phosphatase reduces Ca(2+) sensitivity of contraction and impairs cardiac function. *Circ J* 2010; **74**: 120–128.
  62. Morano I. Effects of different expression and posttranslational modifications of myosin light chains on contractility of skinned human cardiac fibers. *Basic Res Cardiol* 1992; **87**(Suppl 1): 129–141.
  63. van der Velden J, Papp Z, Boontje NM, Zaremba R, de Jong JW, Janssen PM, et al. The effect of myosin light chain 2 dephosphorylation on Ca<sup>2+</sup>-sensitivity of force is enhanced in failing human hearts. *Cardiovasc Res* 2003; **57**: 505–514.
  64. Yu T, Miyagawa S, Miki K, Saito A, Fukushima S, Higuchi T, et al. In vivo differentiation of induced pluripotent stem cell-derived cardiomyocytes. *Circ J* 2013; **77**: 1297–1306.
  65. Hipolito CJ, Suga H. Ribosomal production and in vitro selection of natural product-like peptidomimetics: The FIT and RaPID systems. *Curr Opin Chem Biol* 2012; **16**: 196–203.
  66. Yamagishi Y, Shoji I, Miyagawa S, Kawakami T, Katoh T, Goto Y, et al. Natural product-like macrocyclic N-methyl-peptide inhibitors against a ubiquitin ligase uncovered from a ribosome-expressed de novo library. *Chem Biol* 2011; **18**: 1562–1570.

# Direct comparison of the diagnostic capability of cardiac magnetic resonance and endomyocardial biopsy in patients with heart failure

Akemi Yoshida<sup>1</sup>, Hatsue Ishibashi-Ueda<sup>2</sup>, Naoaki Yamada<sup>3</sup>, Hideaki Kanzaki<sup>1</sup>, Takuya Hasegawa<sup>1</sup>, Hiroyuki Takahama<sup>1</sup>, Makoto Amaki<sup>1</sup>, Masanori Asakura<sup>1,4</sup>, and Masafumi Kitakaze<sup>1,4\*</sup>

<sup>1</sup>Department of Cardiovascular Medicine, National Cerebral and Cardiovascular Center, Suita, Osaka, Japan; <sup>2</sup>Department of Pathology, National Cerebral and Cardiovascular Center, Suita, Osaka, Japan; <sup>3</sup>Department of Radiology, National Cerebral and Cardiovascular Center, Suita, Osaka, Japan; and <sup>4</sup>Department of Clinical Research and Development, National Cerebral and Cardiovascular Center, Suita, Osaka, Japan

Received 19 July 2012; revised 11 September 2012; accepted 30 November 2012

## Aims

The diagnostic performance of cardiac magnetic resonance (CMR) has not been compared with that of other imaging modalities. Therefore, this study investigated the diagnostic capabilities of CMR and endomyocardial biopsy (EMB) in patients with heart failure (HF).

## Methods and results

We studied 136 patients with cardiomyopathy who underwent both CMR and EMB. Independent diagnoses were made according to the results of (i) CMR alone; (ii) EMB alone; (iii) clinical data plus echocardiogram; (iv) clinical data, echocardiogram, plus CMR; and (v) clinical data, echocardiogram, plus EMB. These diagnoses were then compared with the final diagnosis (gold standard) that was made using the complete clinical data, including EMB and CMR. The sensitivities of the diagnosis strategies of (i–v) relative to the final diagnosis were 67, 79, 86, 97, and 100%, respectively. CMR alone demonstrated better sensitivity for cardiac sarcoidosis and greater specificity for dilated cardiomyopathy than EMB alone. CMR also tended to show better sensitivity for hypertensive heart disease. There was no difference between the diagnostic capability of CMR and EMB for hypertrophic cardiomyopathy (HCM). However, CMR showed excellent sensitivity (100%) for apical and obstructive HCM, whereas EMB displayed better sensitivity for dilated HCM. Moreover, combined diagnosis with clinical data, echocardiogram, plus CMR achieved superior agreement with the final diagnosis in comparison with EMB alone.

## Conclusion

Non-invasive CMR demonstrated excellent diagnostic capability for patients with HF and was as effective as or superior to EMB. In particular, the use of CMR in combination with clinical data unrelated to EMB may provide excellent diagnostic accuracy for HF.

## Keywords

Heart failure • CMR • Endomyocardial biopsy • Diagnosis • Aetiology • Cardiomyopathy

## Introduction

Heart failure (HF) is a common clinical syndrome caused by various cardiovascular diseases.<sup>1</sup> Despite the discovery, development, and adoption of novel therapies for HF, the mortality and morbidity resulting from this condition have remained high and

are currently increasing. Accordingly, accurate diagnosis of the underlying aetiology of HF is important for appropriate management and treatment. In addition to conventional clinical methods, gadolinium-enhanced cardiac magnetic resonance (CMR) and endomyocardial biopsy (EMB) are useful diagnostic modalities for identifying the aetiology of HF. EMB is considered

\* Corresponding author. Departments of Clinical Research and Development, and Cardiovascular Medicine, National Cerebral and Cardiovascular Center, 5-7-1 Fujishiro-dai, Suita, Osaka 565-8565, Japan. Tel: +81 6 6833 5012, Fax: +81 6 6836 1120, Email: kitakaze@zf6.so-net.ne.jp

Published on behalf of the European Society of Cardiology. All rights reserved. © The Author 2013. For permissions please email: journals.permissions@oup.com.

to be the gold standard for diagnosing myocarditis as well as certain infiltrative cardiac diseases, such as amyloidosis, sarcoidosis, and haemochromatosis. In contrast, CMR is also required to identify patients with cardiomyopathy accurately, according to the Consensus Panel Report.<sup>2</sup> CMR is a non-invasive, accurate, and reproducible imaging technique that can be used to evaluate cardiac morphology and function, and provide valuable information for tissue characterization. In addition, several studies have suggested that CMR techniques using late-gadolinium enhancement (LGE) are useful for diagnosing various types of cardiomyopathies. Indeed, both CMR and EMB have demonstrated good performance in patients with troponin-positive acute chest pain but without coronary artery disease.<sup>3</sup> However, there have been no reports directly comparing the diagnostic utility of CMR and EMB in patients with HF.

Therefore, we compared the diagnostic capability of CMR and EMB in HF patients and also assessed the diagnostic performance of the combined use of CMR and all clinical data in comparison with EMB alone.

## Methods

### Selection of patients

A total of 1034 consecutive patients with HF of unknown aetiology were evaluated between January 2007 and July 2009. Patients who were admitted to our institution for the management of HF, who had LV hypertrophy and/or LV dysfunction, and who had received EMB and LGE CMR were included in this study. Patients were excluded if they had one or more of the following conditions:

substantial valvular or ischaemic heart disease; congenital heart disease; constrictive pericarditis; idiopathic restrictive cardiomyopathy; an ambiguous final diagnosis; dilated cardiomyopathy (DCM) with an LVEF > 55%; poor-quality CMR; or an inadequate myocardial biopsy. Of the patients examined, 25 were given an ambiguous final diagnosis for the following reasons: 17 patients did not receive sufficient detailed investigations to reach the final diagnosis; 3 patients were suspected as having arrhythmogenic right ventricular cardiomyopathy (ARVC) but they did not fulfil the Task Force Criteria;<sup>4</sup> 3 patients were suspected as having dilated hypertrophic cardiomyopathy (HCM) but hypertrophic stage was not detected; and 2 patients were diagnosed as LV non-compaction and we excluded these patients because EMB cannot diagnose this condition. As a result, we enrolled 136 patients in this study (Figure 1).

For all patients, a careful medical history was collected and physical examinations, laboratory tests, echocardiography, coronary angiography, and right heart catheterization were performed. EMB and CMR were also performed in all patients to evaluate evidence of HF. We identified the aetiology of HF using all possible diagnostic approaches in addition to EMB and CMR.

This study was approved by our Institutional Research Ethics Committee. The Committee decided that informed consent from the 136 subjects was not required according to the Japanese Clinical Research Guidelines because this was a retrospective, observational study. Instead, we made a public announcement as per the request of the Ethics Committee.

### Aetiology of cardiomyopathy

According to the clinical data, echocardiogram, CMR, and EMB, six diagnoses were made for each patient, including (i) CMR diagnosis; (ii) EMB diagnosis; (iii) the combined diagnosis with clinical data

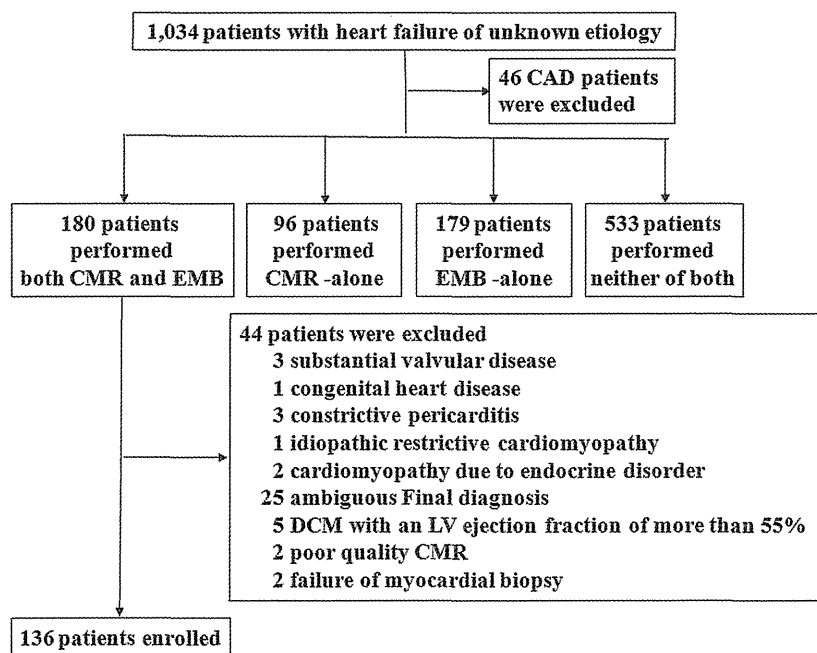


**Figure 1** Study profile. Flow chart of the 1034 consecutive patients with heart failure of unknown aetiology admitted to our institution. The chart shows the immediate exclusion of cardiomyopathy due to significant coronary artery disease (CAD) and the further management of these patients. CMR, cardiac magnetic resonance; DCM, dilated cardiomyopathy; EMB, endomyocardial biopsy.

plus echocardiogram; (iv) the combined diagnosis with clinical data, echocardiogram, plus CMR; (v) the combined diagnosis with clinical data, echocardiogram, plus EMB; and (vi) the final diagnosis. The CMR and EMB diagnoses (i and ii) were established according to the results of CMR or EMB alone, and the investigators were blinded to all of the other data. Clinical data were defined as any method that could be used to diagnose HF other than echocardiography, CMR, or EMB, such as the collection of a patient's medical history, laboratory tests, scintigraphy, and coronary angiography. The final diagnosis (vi) was made prior to patient discharge by an expert team of cardiologists using all of the available data, including the results of EMB, CMR, and other diagnostic modalities. In addition, an expert team of cardiologists, who were not specialists in either CMR or EMB but could interpret these studies, was recruited. The final diagnoses were based on the recommendations of the 2008 European Society of Cardiology (ESC) report for the classification of cardiomyopathies.<sup>5</sup> In patients with several causes of HF, the most significant cause was associated with the diagnosis.

Each diagnosis was assigned according to one of the following categories: DCM, HCM, hypertensive heart disease (HHD), ARVC, muscular dystrophy, infiltrative myocardial disease (i.e. amyloidosis and sarcoidosis), myocarditis, or other causes.

### Cardiac magnetic resonance images and analysis

Images were acquired using a 1.5 T scanner (Sonata, Siemens Medical Solutions, Erlangen, Germany). The CMR protocol consisted of a cardiac functional study, spin-echo imaging, and LGE imaging, as previously described.<sup>6</sup> For the cardiac functional study, three standard long-axis slices and a stack of contiguous short-axis slices (slice thickness, 6 mm; slice gap, 4 mm) were acquired as ECG-gated steady-state free-precession cine images with radial scans and breath-holding. T2-weighted spin-echo images were acquired using half-Fourier acquisition single shot turbo spin-echo (HASTE) before contrast injection with an echo time of 82 ms and fat saturation in the same position as the cine images. LGE images were acquired in the same positions as the cine images at 2, 5, 10, and 20 min after i.v. injection of 0.15 mmol/kg of gadolinium-diethyltriaminepentaacetic acid. The inversion delay time was 300 ms.

The cine and LGE images were evaluated by several observers who were blinded to the clinical data. The EF and volumes were measured quantitatively for the left and right ventricles according to the end-diastolic and end-systolic endocardial contours from a stack of short-axis cine images using ARGUS software. The LV mass (LVM) was calculated as the total myocardial volume multiplied by the specific gravity of the myocardium (1.05 g/mL). The ventricular end-diastolic and end-systolic volumes (EDV and ESV, respectively) and the LVM were standardized according to the body surface area ( $m^2$ ). The presence, location, and extent of LGE were determined using a standard 17 segment LV model.<sup>7</sup> We classified the pattern of enhancement as subendocardial, midwall (longitudinal stripes), subepicardial, or transmural, as well as patchy (focal enhancement not following the coronary vascular territories) or diffuse.

### Endomyocardial biopsy and analysis

Biopsy specimens were taken from the endocardium at the right inter-ventricular septum using Technowood disposable biopsy forceps (TONOKURA IKA KOGYO CO., LTD, Tokyo, Japan) via the right internal jugular vein or right femoral vein, as described elsewhere.<sup>8</sup> Three to five specimens were obtained from each patient. No complications related to EMB were observed. Biopsy specimens were

immediately fixed in 15% formalin for 24 h, embedded in paraffin, and cut into 4  $\mu$ m thick sections. The sections were stained with haematoxylin and eosin and Masson's trichrome. Some of the EMB specimens were frozen for polymerase chain reaction (PCR) analysis for the detection of enterovirus when myocarditis was suspected. Congo red staining was added when amyloidosis was suspected. Immunohistochemistry was performed in ARVC, myocarditis, amyloidosis, dystrophic cardiomyopathy, and some cases of HCM, as appropriate.

While EMB analysis at final diagnosis was made as above using all of the other data, EMB diagnosis was evaluated using only haematoxylin and eosin and Masson's trichrome stains by several cardiac pathologists who were not aware of the clinical features of the patients in this study.

### Diagnosis of cardiomyopathy by cardiac magnetic resonance or endomyocardial biopsy

The diagnosis of cardiomyopathy by CMR and EMB was based on well-established and widely accepted definitions.<sup>9,10</sup> A CMR diagnosis was made according to the dimensions, regional and global wall motion, wall thickness, and the presence and pattern of LGE,<sup>11–14</sup> whereas an EMB diagnosis was made according to the report for classification of cardiomyopathies.<sup>4,5,15,16</sup>

A histological diagnosis of DCM was performed by examining the following criteria: interstitial fibrosis, replacement fibrosis, inflammatory cell infiltrates, cellular hypertrophy, and myocardial cell degeneration.<sup>17</sup> Histopathological criteria for HCM included severe myocyte hypertrophy, myocyte disarray > 10%, plexiform fibrosis, and nuclear hypertrophy. The diagnosis of HHD was made according to the presence of moderate myocyte hypertrophy,<sup>18</sup> interstitial fibrosis, and the lack of myocyte disarray. The presence of non-caseating epithelioid granulomas with giant cells was considered indicative of cardiac sarcoidosis (CS).<sup>16</sup> The diagnosis of myocarditis was based on the Dallas criteria modified by the Japanese Circulation Society Guidelines.<sup>19</sup> Based on this modified version of the Dallas criteria, the immunohistochemistry was used to characterize the inflammatory infiltrates. The cut-off for mononuclear cell infiltrates was an inflammatory infiltrate count of at least 5/high power field. We confirmed the diagnoses of cardiac amyloidosis by electron microscopy and performed immunohistochemistry for amyloid typing. The histology diagnosis for ARVC was made according to the Task Force Criteria.<sup>4</sup>

The characteristics of DCM for CMR included dilation and impaired contraction of one or both ventricles and an LVEF < 55%.<sup>20</sup> Moreover, the wall thickness is normal or decreased. HCM is characterized by hypertrophy of the left ventricle and occasionally the right ventricle, normal or reduced LV volume, and normal LV contraction or hypercontraction. Apical HCM was regarded as hypertrophy of the apex, and hypertrophic obstructive cardiomyopathy (HOCM) was regarded as an obstruction to the LV outflow tract. We defined dilated HCM as an LVEF  $\leq$  50%<sup>21,22</sup> and evidence of wall thickening prior to the study. Generally, dilated HCM is characterized by a relative wall thickness with a dilated LV cavity. LV hypertrophy is common in HHD, and additional common findings include a relative wall thickness with or without a dilated LV cavity. The use of CMR for CS can demonstrate certain characteristic features, such as septal thinning, ventricular dilatation, segmental systolic dysfunction, global systolic dysfunction, or ventricular aneurysm. We referred to the typical LGE pattern for diagnosis of DCM, HCM, HHD, and CS. The typical LGE pattern regarded a DCM LGE pattern as patchy or longitudinal midwall enhancement, a HCM LGE pattern as patchy and located at the LV–RV junction, a CS LGE pattern as a non-ischaemic pattern with enhancement of the midwall or epicardium at various sites, especially the anteroseptal

and inferolateral walls, and a HHD LGE pattern as similar to the DCM LGE pattern based upon a previous report.<sup>10</sup> Myocarditis was diagnosed when subepicardial and midwall areas demonstrated an increased signal in the T2-weighted image or when the lateral and inferolateral walls demonstrated an LGE distribution in the epicardium toward the mid myocardial wall. ARVC is characterized by regional or global dysfunction, dilatation, and focal aneurysm of the right ventricle noted in the 2010 guideline,<sup>4</sup> whereas amyloidosis is characterized by concentric hypertrophy with normal or reduced contractility, a thickened interatrial septum, bi-atrial dilation, and a circumferential pattern of LGE, preferentially involving the subendocardium but occasionally demonstrating a patchy transmural pattern. Dystrophic cardiomyopathy in LGE preserves the subendocardium and is more frequently located in the LV lateral wall.

### Statistical analysis

Continuous variables were expressed as the mean  $\pm$  standard deviation (SD), whereas categorical variables were expressed as numbers and percentages. Comparisons between groups were performed using a two-sample *t*-test for normally distributed continuous variables and the Wilcoxon test for variables that did not demonstrate a normal distribution. For categorical variables, we used the  $\chi^2$  test and Fisher's exact test, as appropriate. For each type of cardiomyopathy, the sensitivity, specificity, diagnostic accuracy, positive predictive value (PPV), negative predictive value (NPV), and 95% confidence interval (CI) for the CMR diagnosis, EMB diagnosis, and combined diagnosis with clinical data, echocardiogram, plus CMR were calculated in comparison with the final diagnosis, which served as the gold standard. The PPV and NPV were computed using the following formulae:  $PPV = \text{true positive}/(\text{true positive} + \text{false positive})$ ; and  $NPV = \text{true negative}/(\text{true negative} + \text{false negative})$ . Diagnostic accuracy was calculated using the following formulae:  $\text{diagnostic accuracy} = (\text{true positive} + \text{true negative})/\text{total}$ . A comparison of the diagnostic methods was performed using McNemar's test. The analyses were performed using JMP version 7 statistical software. All of the presented 95% CI are two.

## Results

### Study population and patient characteristics

A total of 136 patients were studied (Supplementary material, Table S1). The mean age of these patients was  $52 \pm 17$  years (range 16–81 years): 83 of the patients were male, and 18 patients suffered from AF. EMB and CMR with LGE were performed in all patients, and none of the 136 patients was diagnosed with significant coronary artery disease. The most common diagnosis was DCM (54 patients, 40%), which was followed by HCM (36 patients, 26%). The remaining 46 patients were diagnosed with a secondary cardiomyopathy or HHD. The HCM patients included 4 cases of apical hypertrophy, 11 cases of HOCM, and 15 cases of HCM in the dilated phase.

The CMR results revealed asymmetric septal hypertrophy (septal/free wall thickness ratio  $\geq 1.3$ ) in 25 patients (18%), most of whom had either HCM (84%) or HHD (12%) detailed in the Supplementary material, Table S1.

The median patient follow-up period was 655 days (range 243–1143 days), and no diagnoses were changed during this time.

### Comparison between cardiac magnetic resonance, endomyocardial biopsy, and the combined diagnosis

The sensitivity of EMB, CMR, and the combined diagnosis with clinical data plus echocardiogram, with clinical data, echocardiogram, plus CMR, and with clinical data, echocardiogram, plus EMB was 67, 79, 86, 97, and 100% relative to the final diagnosis, respectively. Table 1 shows the diagnostic performance of CMR, EMB, and the combined diagnosis with clinical data, echocardiogram, plus CMR. The use of CMR demonstrated a diagnostic capability comparable with EMB for all causes of HF. The highest level of sensitivity of EMB was for DCM (89%) followed by HCM (75%) and HHD (36%) (Table 2), whereas the greatest sensitivity of CMR was observed for DCM (83%) followed by HCM (81%) and CS (76%). Furthermore, to explore the relative merits of CMR vs. EMB, we investigated indications of EMB noted in the 2007 guidelines.<sup>23</sup> EMB demonstrated a better diagnostic yield for DCM and dilated HCM, whereas CMR demonstrated better diagnostic performance for cases of CS and HHD even when the indication for EMB was a class I. The diagnostic analysis is listed in Table 3. We gave six patients with dilated HCM an incorrect diagnosis of CS and also gave five patients with HHD an incorrect diagnosis of DCM using CMR. In contrast, we tended to misdiagnose CS and HHD as DCM and HCM as HHD when using EMB. Specifically, the six patients with HCM who were misdiagnosed for HHD by EMB included three patients with HOCM diagnoses, two with apical HCM diagnoses, and one with a diagnosis of dilated HCM. Table 2 shows the sensitivity and specificity for the use of EMB, CMR, and the combined diagnosis with clinical data, echocardiogram, plus CMR. Overall, CMR demonstrated increased specificity for DCM compared with EMB, and CMR also tended to be more sensitive for the diagnosis of CS and HHD. In contrast, EMB demonstrated lower sensitivity than CMR for most diagnoses, with the exception of DCM.

We also examined the diagnostic accuracy of CMR, EMB, and the combined diagnosis with clinical data, echocardiogram, plus CMR (Table 2). The sensitivity of the combined diagnosis with clinical data, echocardiogram, plus CMR was greater than that of EMB for the detection of HCM, CS, and HHD. The agreement of both CMR and EMB with a final diagnosis of DCM, HCM, CS, and HHD was noted to be 72, 58, 23, and 21%, respectively (Figure 2). Conversely, both CMR and EMB misdiagnosed 6, 3, 12, and 21% of patients with DCM, HCM, CS, and HHD, respectively. Importantly, all of the patients who received accurate diagnoses with EMB alone were also correctly diagnosed using the combined diagnosis with clinical data, echocardiogram, plus CMR.

### Characteristics and details of cardiac magnetic resonance

We analysed the frequency of the use of the typical LGE pattern only in cases in which we diagnosed DCM, HCM, CS, and HHD. The CMR results revealed a DCM LGE pattern, HCM LGE pattern, CS LGE pattern, or HHD LGE pattern in 78, 53, 82, and 79% of the patients with DCM, HCM, CS, and HHD, respectively (Figure 3). In addition, the patients with typical LGE patterns were more likely to receive an accurate diagnosis. LGE in the papillary

**Table 1 Agreement of endomyocardial biopsy, cardiac magnetic resonance, or combined diagnosis with clinical data, echocardiogram, plus cardiac magnetic resonance with final diagnosis in 136 patients based on endomyocardial biopsy indication**

Final diagnoses, n EMB indication (class)	Number		EMB diagnosis, n (%)		CMR diagnosis, n (%)		Combined diagnosis, n (%)
	I	IIa/IIb	I	IIa/IIb	I	IIa/IIb	
DCM, 54	30	24	26 (87)	22 (92)	24 (80)	21 (88)	51 (94)
HCM, 36	11	25	7 (64)	20 (80)	6 (55)	23 (92)	35 (97)
Dilated HCM, 15	9	6	7 (78)	5 (83)	4 (44)	5 (83)	15 (100)
Obstructive HCM, 11	0	11	0 (0)	9 (82)	0 (0)	11 (100)	11 (100)
Apical HCM, 4	0	4	0 (0)	2 (50)	0 (0)	4 (100)	4 (100)
Sarcoidosis, 17	8	9	2 (25)	4 (44)	6 (75)	7 (78)	17 (100)
HHD, 14	5	9	2 (40)	3 (33)	5 (100)	4 (44)	14 (100)
Others							
ARVC, 5	1	4	0 (0)	0 (0)	1 (100)	4 (100)	5 (100)
Myocarditis, 4	4	0	3 (75)	0 (0)	1 (25)	0 (0)	4 (100)
Amyloidosis, 3	0	3	0 (0)	2 (67)	0 (0)	3 (100)	3 (100)
Dystrophic cardiomyopathy, 3	1	2	0 (0)	0 (0)	1 (100)	2 (100)	3 (100)
Total	60	76	40 (67)	51 (67)	44 (73)	64 (84)	132 (97)

ARVC, arrhythmogenic right ventricular cardiomyopathy; CMR, cardiac magnetic resonance; DCM, dilated cardiomyopathy; EMB, endomyocardial biopsy HCM, hypertrophic cardiomyopathy; HHD, hypertensive heart disease.

muscle was frequently found in patients with HCM or sarcoidosis, while it was rarely or never seen in patients with DCM or HHD.

## Discussion

This was the first study to compare the diagnostic performance of EMB and CMR in patients with HF. Non-invasive CMR, especially when combined with clinical data and echocardiogram, may provide an excellent diagnostic capacity for identifying the underlying aetiology in patients with HF, equal to or better than invasive EMB. Moreover, CMR is a powerful modality which in combination with clinical data including echocardiogram is sufficient for defining the pathophysiology of HF.

Although it is important to compare the diagnostic potential of EMB and CMR across a large number of patients with HF, comparisons using a large population have not been possible because it is extremely difficult to perform both EMB and CMR with LGE in sufficient patients. Our findings revealed that both the invasive EMB technique and the non-invasive CMR technique demonstrated good diagnostic performance (67% vs. 79%), whereas the use of CMR in combination with clinical data including echocardiogram unrelated to the EMB findings demonstrated excellent diagnostic performance (97%). Importantly, CMR alone could not surpass the diagnostic accuracy of EMB, which underscores the importance of EMB. However, the combined diagnosis was more accurate, which suggests that the use of CMR in combination with clinical data plus echocardiogram is the most reliable, non-invasive method for the diagnosis of HF in a routine clinical setting. Thus, we concluded that CMR is equal to or possibly superior to the use of EMB for the diagnosis of the underlying aetiology of HF,

especially in patients with sarcoidosis, HHD, others, and those with a class II indication for EMB.

These results suggest that CMR should be used more often than EMB for the initial diagnosis of HF. In addition, the cost of EMB is approximately three times greater than that of delayed enhancement CMR, and most patients can receive CMR at a clinic but would require a hospital stay to undergo EMB and perform EMB with right heart catheterization (which also contributes to the high cost of EMB). Indeed, the 2009 American College of Cardiology (ACC)/American Heart Association (AHA) chronic HF guidelines proposed that EMB should not be performed for the routine evaluation of patients with HF,<sup>24</sup> as EMB is often associated with sampling errors and complications. Therefore, although we do not deny the usefulness of EMB for the diagnosis of the underlying aetiology of HF, we suggest that CMR should be used more frequently for this type of diagnosis.

## Diagnostic performance of cardiac magnetic resonance and endomyocardial biopsy

Although EMB provides suggestive findings in patients with DCM, HHD, and dystrophic cardiomyopathy, these findings are non-specific, and a definitive diagnosis cannot be made by EMB *per se*. In contrast, cardiac amyloidosis, CS, HCM, and myocarditis have specific histological characteristics and can be conclusively diagnosed using EMB alone if myocardial biopsy specimens contain these lesions (Figure 4). In our study, an accurate and conclusive diagnosis of such conditions could be reached using EMB alone in 38 out of 60 patients (Table 1), and we tended to misdiagnose CS and HHD as DCM, and HCM as HHD by EMB (Table 3).

**Table 2 Sensitivity, specificity, positive predictive value, negative predictive value, accuracy of cardiac magnetic resonance diagnosis, and combined diagnoses with clinical data, echocardiogram, plus cardiac magnetic resonance vs. endomyocardial biopsy diagnosis**

A. Cardiac magnetic resonance vs. endomyocardial biopsy												
	n	Sensitivity		rTPF	95% CI	n	Specificity		rFPF	95% CI		
		CMR	EMB				CMR	EMB				
DCM	54	83%	<b>89%</b>	1.07	0.89–1.28	82	<b>93%</b>	69%	<b>4.3</b>	<b>1.72–10.7</b>		
HCM	36	<b>81%</b>	75%	0.93	0.69–1.26	100	<b>98%</b>	94%	3	0.48–18.64		
CS	17	<b>76%</b>	35%	0.46	0.20–1.07	119	92%	<b>100%</b>	<b>0</b>	–		
HHD	14	<b>64%</b>	36%	0.56	0.22–1.43	122	<b>96%</b>	92%	2	0.59–6.81		

B. Cardiac magnetic resonance vs. endomyocardial biopsy												
	n	PPV		rPPV	95% CI	n	NPV		rNPV	95% CI	Accuracy	
		CMR	EMB				CMR	EMB			CMR	EMB
DCM	54	<b>88%</b>	66%	<b>0.75</b>	<b>0.60–0.93</b>	82	89%	<b>90%</b>	1.01	0.89–1.15	<b>89%</b>	75%
HCM	36	<b>94%</b>	82%	0.87	0.71–1.08	100	<b>93%</b>	91%	0.98	0.89–1.07	<b>93%</b>	89%
CS	17	57%	<b>100%</b>	<b>1.77</b>	<b>1.18–2.66</b>	119	<b>96%</b>	92%	0.95	0.88–1.02	90%	<b>92%</b>
HHD	14	<b>64%</b>	33%	0.52	0.20–1.31	122	<b>96%</b>	93%	0.97	0.90–1.04	<b>93%</b>	86%

C. Combined procedure using clinical data with echocardiogram plus cardiac magnetic resonance vs. endomyocardial biopsy												
	n	Sensitivity		rTPF	95% CI	n	Specificity		rFPF	95% CI		
		Combined	EMB				Combined	EMB				
DCM	54	<b>94%</b>	89%	0.94	0.82–1.08	82	<b>100%</b>	69%	–	–		
HCM	36	<b>97%</b>	75%	<b>0.77</b>	<b>0.61–0.97</b>	100	<b>99%</b>	94%	6	0.54–67.19		
CS	17	<b>100%</b>	35%	<b>0.35</b>	<b>0.17–0.74</b>	119	99%	<b>100%</b>	0	–		
HHD	14	<b>100%</b>	36%	<b>0.36</b>	<b>0.16–0.80</b>	122	<b>98%</b>	92%	5	0.88–28.27		

D. Combined procedure using clinical data with echocardiogram plus cardiac magnetic resonance vs. endomyocardial biopsy												
	n	PPV		rPPV	95% CI	n	NPV		rNPV	95% CI	Accuracy	
		Combined	EMB				Combined	EMB			Combined	EMB
DCM	54	100%	66%	<b>0.65</b>	<b>0.52–0.81</b>	82	<b>96%</b>	90%	0.94	0.85–1.03	<b>98%</b>	75%
HCM	36	<b>97%</b>	82%	0.84	0.69–1.02	100	<b>99%</b>	91%	<b>0.92</b>	<b>0.86–0.99</b>	<b>99%</b>	89%
CS	17	<b>94%</b>	100%	1.06	0.93–1.20	119	<b>100%</b>	92%	<b>0.92</b>	<b>0.86–0.97</b>	<b>99%</b>	92%
HHD	14	<b>88%</b>	33%	<b>0.38</b>	<b>0.16–0.89</b>	122	<b>100%</b>	93%	<b>0.93</b>	<b>0.87–0.98</b>	<b>99%</b>	86%

CI, confidence interval; CMR, cardiac magnetic resonance; CS, cardiac sarcoidosis; DCM, idiopathic dilated cardiomyopathy; EMB, endomyocardial biopsy; FPF, false positive fraction; HCM, hypertrophic cardiomyopathy; HHD, hypertensive heart disease; NPV, negative predictive value; PPV, positive predictive value; TPF, true positive fraction. 95% CIs were calculated according to the ratio of CMR diagnosis and combined diagnosis to EMB diagnosis. The bold values indicate a significant difference.

These misdiagnoses were attributed to non-specific changes in the biopsy specimens or the inappropriate sampling of sites separate from the lesions due to the patchy distribution of the lesions.<sup>17,25–27</sup> However, there are merits in the classification of infiltrating inflammatory cells by either immunohistochemistry or a PCR method to guide treatment. The ESC 2012 guidelines also stated that the use of EMB may be needed to confirm the diagnosis in patients with suspected myocarditis, sarcoidosis, and amyloidosis.<sup>1</sup>

Cardiac magnetic resonance is a safe procedure, and images of diagnostic quality can be obtained in ≥ 98% of patients.<sup>28</sup> The use of CMR also allowed us to obtain detailed images of not

only functional and morphological abnormalities but also tissue pathology. In this study, EMB was superior to CMR for diagnoses of DCM and dilated HCM, whereas CMR demonstrated an improved diagnostic yield over EMB in cases of non-dilated HCM, CS, HHD, and other rare diseases (with the exception of myocarditis). Moreover, this tendency was the same independent of the EMB indication. In contrast to previous studies demonstrating a high level of sensitivity and specificity within only a limited study population, our study observed lower diagnostic agreement between methods. Because CMR was used to differentiate between a broad spectrum of diagnostic characteristics in HF patients, which resembles the clinical setting, CMR alone could

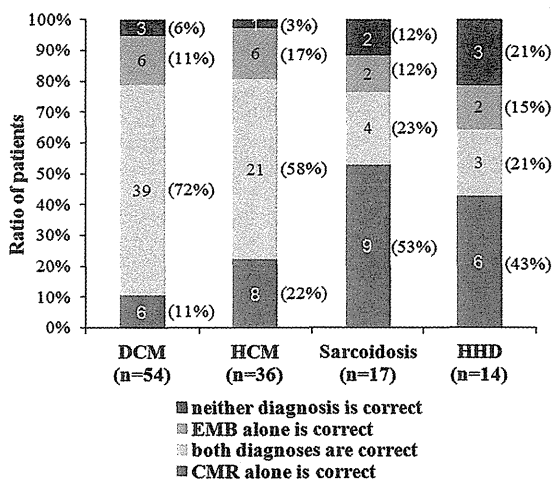
**Table 3 Comparison of cardiac magnetic resonance diagnosis or endomyocardial biopsy diagnosis with final diagnosis**

Final diagnosis	CMR diagnosis	DCM (n = 54)	HCM (n = 36)	CS (n = 17)	HHD (n = 14)	Others (n = 15)
DCM, n (%)		<b>45 (83)</b>	0	1	5 (36)	0
HCM, n (%)		1	<b>29 (81)</b>	1	0	0
CS, n (%)		2 (4)	6 (17)	<b>13 (76)</b>	0	2 (13)
HHD, n (%)		3 (5)	1	0	<b>9 (64)</b>	0
Others, n (%)		3 (5)	0	2 (12)	0	<b>12 (80)</b>

Final diagnosis	EMB diagnosis	DCM (n = 54)	HCM (n = 36)	CS (n = 17)	HHD (n = 14)	Others (n = 15)
DCM, n (%)		<b>48 (89)</b>	3 (8)	10 (59)	7 (50)	6 (40)
HCM, n (%)		3 (6)	<b>27 (75)</b>	0	2 (14)	1 (7)
CS, n (%)		0	0	<b>6 (35)</b>	0	0
HHD, n (%)		2 (4)	6 (17)	0	<b>5 (36)</b>	2 (13)
Others, n (%)		1	0	1	0	<b>5 (33)</b>

The bold values indicate diagnostic concordance between cardiac magnetic resonance diagnosis or endomyocardial biopsy diagnosis and final diagnosis.



**Figure 2** Diagnostic capabilities of endomyocardial biopsy (EMB), cardiac magnetic resonance (CMR), and the combined diagnosis with CMR and EMB. DCM, idiopathic dilated cardiomyopathy; HCM, hypertrophic cardiomyopathy; CS, cardiac sarcoidosis; HHD, hypertensive heart disease. The ratio between EMB and CMR for the diagnosis of DCM, HCM, CS, and HHD.

not assign a correct diagnosis for 28 patients (21%) (Table 1). The use of CMR tended to misdiagnose HCM as CS, and HHD as DCM. Additionally, six HCM patients who were misdiagnosed with CS all had dilated HCM. A study by Hansen *et al.* suggested that the use of CMR in CS patients demonstrates similar results to those obtained in patients with HCM or idiopathic cardiomyopathy,<sup>29</sup> which is consistent with the present data (Table 3). In the five cases where HHD was misdiagnosed, they were consistently misdiagnosed as DCM due to the similarity of the images.<sup>10</sup> However, in HCM patients, CMR demonstrated excellent

diagnostic performance (100%) for apical HCM and HOCM, which suggests that CMR has the ability to evaluate the heterogeneous appearance of HCM better than any other imaging modality,<sup>30,31</sup> and this represents the main difference between CMR and EMB. We could not refer to the diagnostic accuracy of CMR in patients with myocarditis in our study because the number with myocarditis was too small. On the other hand, Marvorigeni *et al.* importantly concluded that both CMR and PCR prove useful for the detection of myocarditis, while CMR is important to detect the development of HF.<sup>32</sup> Our data are consistent with the previous study<sup>32</sup> showing that CMR and EMB have equivalent ability to reach the diagnosis and judge the pathophysiology.

Although the merits and demerits of CMR differ from those of EMB, its diagnostic capability was shown to be equivalent or even superior to that of EMB.

### Superiority of the combined diagnosis

The combined diagnosis with non-invasive clinical data provides a sharp impact on an accurate diagnosis of HF.<sup>33</sup> Likewise, the combined diagnosis with clinical data, echocardiogram, plus CMR was shown to be very effective in the current study. Out of 54 DCM patients, 9 were misdiagnosed by CMR, but 6 of these 9 patients were correctly diagnosed using the combined diagnostic technique. Of 36 HCM patients, 7 were misdiagnosed by CMR, although 6 of these 7 patients were correctly assessed using the combined diagnosis (Tables 2 and 3). Moreover, the other misdiagnosed patients were also correctly assessed using the combined diagnosis.

Regarding the combined diagnosis with echocardiogram, the present study suggests that even the use of only clinical characteristics including echocardiogram can provide relatively high diagnostic performance compared with that in a previous report,<sup>33</sup> since our Department is specialized in diagnosing patients with non-ischaemic HF. However, the addition of CMR and EMB on top of the clinical information with echocardiogram increases the accuracy to 97% and 100%, respectively. Our original conclusion



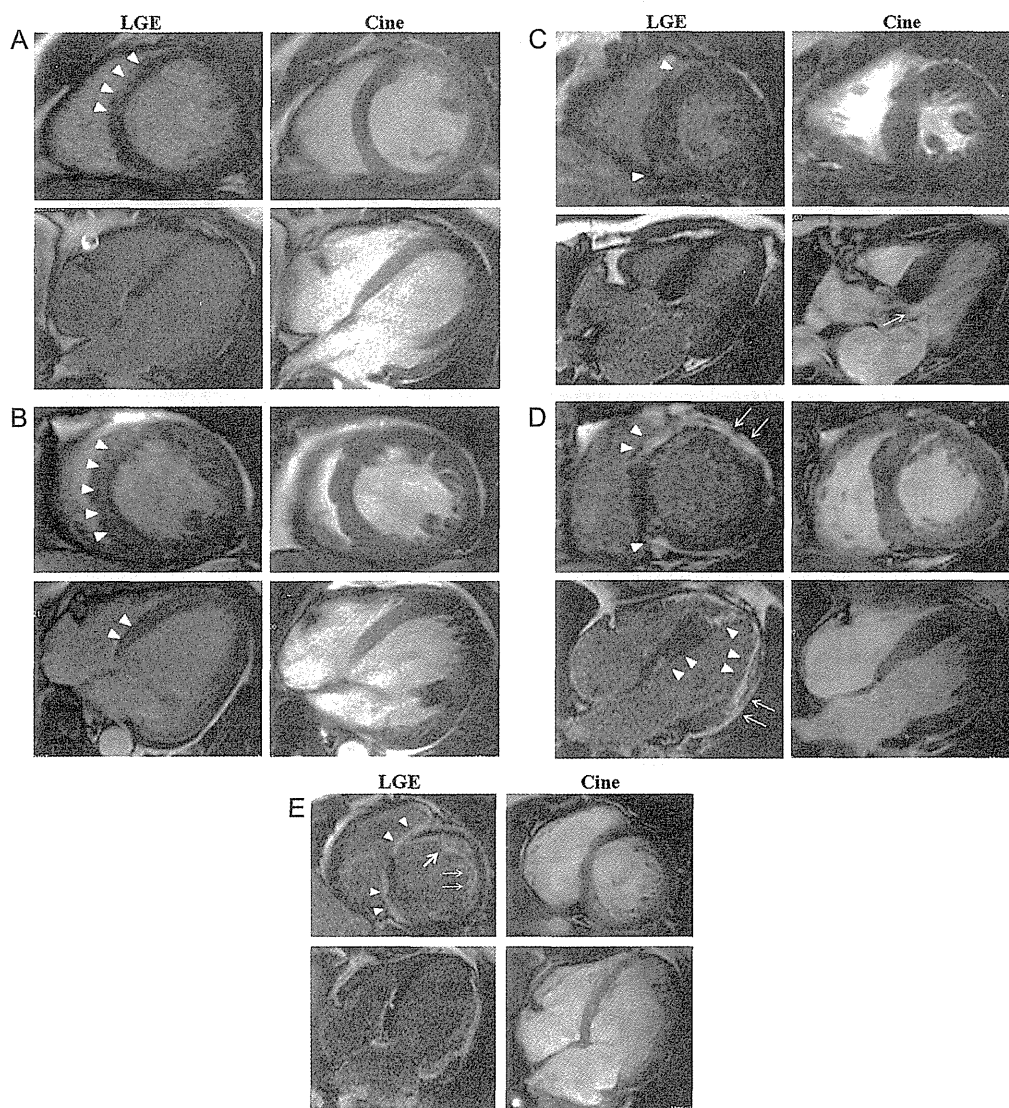


**Figure 3** Representative cardiac magnetic resonance (CMR) findings. (A) Dilated cardiomyopathy (DCM): midwall longitudinal thin late-gadolinium enhancement (LGE) in the anteroseptum wall without wall thickening (arrowheads). (B) Hypertensive heart disease (HHD): broad, ill-defined, and mild LGE in the midwall of the septum (arrowheads) with LV concentric hypertrophy. (C) Hypertrophic obstructive cardiomyopathy (HOCM): LGE in the LV–RV junctions of the anteroseptum and inferoseptum (arrowheads). Note: left atrial dilatation, LV asymmetric hypertrophy, papillary muscle hypertrophy, and LV outflow tract obstruction (arrow). (D) Dilated phase HCM: midwall patchy LGE in the anteroseptum and inferoseptum (arrowheads) and epicardial LGE in the anterior and posterior regions (arrow). (E) Cardiac sarcoidosis: subepicardial LGE of the anteroseptum with wall thinning and inferoseptum (arrowheads), subendocardial LGE of the lateral region (thin arrow), and LGE in the papillary muscle (thick arrow).

that CMR provides a diagnostic capability comparable with EMB seems to be true even with the clinical information including echocardiogram. Furthermore, all of the patients who were correctly diagnosed by EMB were correctly diagnosed using the combined technique, which indicates that the combined method was superior to the use of EMB in this study. Previous studies performed in populations with only one clinically suspected disease reported high diagnostic accuracy,<sup>11,12,34</sup> and our results indicate that CMR would probably be available for a broad spectrum of HF patients, particularly those with a class II indication for EMB, for

differentiation between unknown aetiologies. Furthermore, the knowledge of diseases that are prone to misdiagnosis would increase the diagnostic performance for determining the aetiology of HF in a routine clinical setting. Although CMR is a non-invasive method, as is an echocardiogram, it is equal or superior to an echocardiogram because it can provide specific tissue characterization in addition to cardiac morphology and function. Accordingly, we suggest that it would be better initially to perform CMR in all patients, especially those with a class II indication for EMB, and diagnose the underlying aetiology of HF through the use of

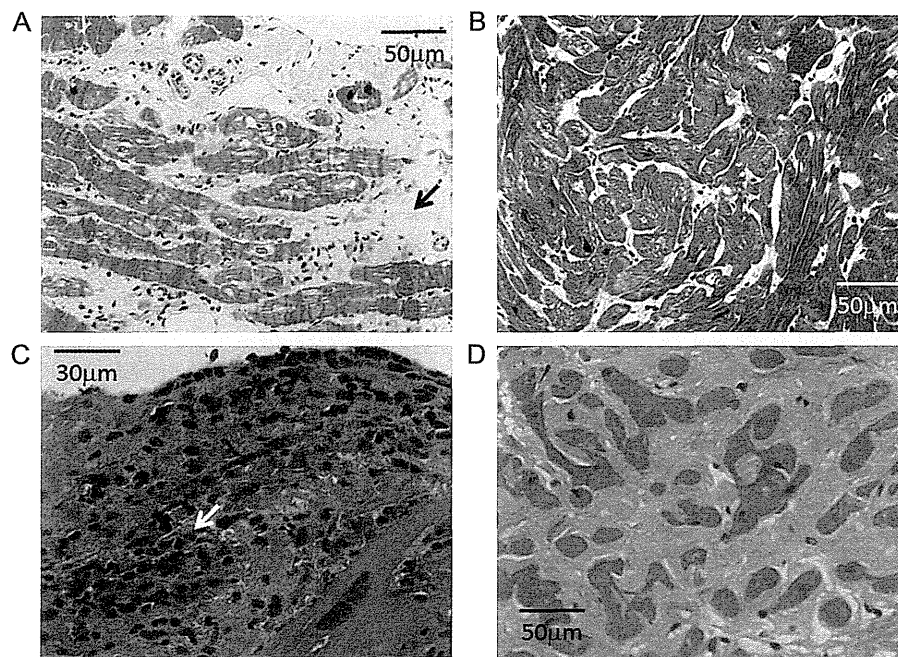


**Figure 4** Representative examples of histological findings from endomyocardial biopsies. (A) Dilated cardiomyopathy (DCM): the photomicrograph demonstrates replacement fibrosis (blue areas, black arrow) and moderate myocyte hypertrophy (Masson trichrome stain, bar = 50  $\mu\text{m}$ ). (B) Hypertrophic cardiomyopathy (HCM): severe hypertrophy of myocytes, myocyte disarray, and bizarre nuclei are shown (Masson trichrome stain, bar = 50  $\mu\text{m}$ ). (C) Cardiac sarcoidosis: non-caseating epithelioid granulomas with giant cells (white arrow) are shown (haematoxylin and eosin stain, bar = 30  $\mu\text{m}$ ). (D) Cardiac amyloidosis: amorphous amyloid deposits (blue-grey) in the perimyocytes were consistent with amyloidosis in the interstitium of the myocardium (Masson's trichrome, bar = 50  $\mu\text{m}$ ).

CMR and other non-invasive modalities. Then, if the combined diagnosis fails, EMB can be used as a second diagnostic modality.

### Study limitations

This study had several limitations. First, all of the patients with HF of unknown aetiology were not assigned to receive both EMB and CMR; EMB was performed to reveal the underlying aetiology of HF, according to the Scientific Statement,<sup>23</sup> whereas CMR was performed in all patients without contraindications for CMR. Secondly, we included patients admitted to the Department with HF, and there were remarkably few patients in our Department who had coronary artery disease. However, even if such patients had been included, CMR would have probably been more useful to diagnose prior myocardial infarction due to spontaneous recanalization or coronary vasospasm than EMB. Thirdly, in the clinical setting, there are always cases with an ambiguous diagnosis despite a detailed investigation. We excluded these cases primarily on the premise that we would achieve a more precise diagnostic yield by avoiding these cases. Regarding EMB procedures, we took 3–5 biopsy specimens for each patient in our study, in accordance with the appropriate guidelines.<sup>23</sup> Additionally, all samples were taken from the right ventricle according to the protocol of our facility. In most patients, we took five samples to decrease sampling error, although the sampling number was decreased to three specimens in patients with both a pre-existing LBBB with a high risk for developing complete atrioventricular

block<sup>8</sup> and obvious idiopathic DCM. The collection of samples from both ventricles may have increased the significance of the findings, but we collected the minimum requirement to decrease the procedural risk of EMB. Finally, this was also a retrospective study from a single centre. Our findings must be carefully interpreted and should be replicated in a prospective, large, multicentre investigation. Despite these limitations, our study has important strengths, such as the inclusion of a sufficient number of patients administered both EMB and CMR, a more precise final diagnosis using all available data, and broad clinical applications.

### Supplementary material

Supplementary material is available at *European Journal of Heart Failure* online.

### Funding

The Ministry of Health, Labor, and Welfare-Japan (grants-in-aid H23-Nanchi-Ippan-22 to M.K.), the Ministry of Education, Culture, Sports, Science and Technology-Japan (grants-in-aid 21390251 to M.K.), the Japan Heart Foundation (grants to M.K.), the Japan Cardiovascular Research Foundation (grants to M.K.).

**Conflict of interest:** none declared.

## References

- McMurray JJ, Adamopoulos S, Anker SD, Auricchio A, Bohm M, Dickstein K, Falk V, Filippatos G, Fonseca C, Gomez-Sanchez MA, Jaarsma T, Kober L, Lip GY, Maggioni AP, Parkhomenko A, Pieske BM, Popescu BA, Ronnevik PK, Rutten FH, Schwitzer J, Seferovic P, Stepinska J, Trindade PT, Voors AA, Zannad F, Zeiher A, Bax JJ, Baumgartner H, Ceconi C, Dean V, Deaton C, Fagard R, Funck-Brentano C, Hasdai D, Hoes A, Kirchhof P, Knuuti J, Kolh P, McDonagh T, Moulin C, Reiner Z, Sechtem U, Sirnes PA, Tendera M, Torbicki A, Vahanian A, Windecker S, Bonet LA, Avraamides P, Ben Lamin HA, Brignole M, Coca A, Cowburn P, Dargie H, Elliott P, Flachskampf FA, Guida GF, Hardman S, Iung B, Merkely B, Mueller C, Nanas JN, Nielsen OW, Orn S, Parissis JT, Ponikowski P. ESC guidelines for the diagnosis and treatment of acute and chronic heart failure 2012: the Task Force for the Diagnosis and Treatment of Acute and Chronic Heart Failure 2012 of the European Society of Cardiology. Developed in collaboration with the Heart Failure Association (HFA) of the ESC. *Eur J Heart Fail* 2012;**14**:803–869.
- Pennell DJ, Sechtem UP, Higgins CB, Manning WJ, Pohost GM, Rademakers FE, Rossum ACv, Shaw LJ, Yucel EK. Clinical indications for cardiovascular magnetic resonance (CMR): Consensus Panel report. *Eur Heart J* 2004;**25**:1940–1965.
- Baccouche H, Mahrholdt H, Meinhardt G, Merher R, Voehringer M, Hill S, Klingel K, Kandolf R, Sechtem U, Yilmaz A. Diagnostic synergy of non-invasive cardiovascular magnetic resonance and invasive endomyocardial biopsy in troponin-positive patients without coronary artery disease. *Eur Heart J* 2009;**30**:2869–2879.
- Marcus FI, McKenna WJ, Sherrill D, Basso C, Baucé B, Bluemke DA, Calkins H, Corrado D, Cox MG, Daubert JP, Fontaine G, Gear K, Hauer R, Nava A, Picard MH, Protonotarios N, Saffitz JE, Sanborn DM, Steinberg JS, Tandri H, Thiene G, Towbin JA, Tsatsopoulou A, Wichter T, Zareba W. Diagnosis of arrhythmogenic right ventricular cardiomyopathy/dysplasia: proposed modification of the Task Force Criteria. *Eur Heart J* 2010;**31**:806–814.
- Elliott P, Andersson B, Arbustini E, Bilinska Z, Cecchi F, Charron P, Dubourg O, Kuhl U, Maisch B, McKenna WJ, Monserrat L, Pankuweit S, Rapezzi C, Seferovic P, Tavazzi L, Keren A. Classification of the cardiomyopathies: a position statement from the European Society of Cardiology Working Group on Myocardial and Pericardial Diseases. *Eur Heart J* 2008;**29**:270–276.
- Kono AK, Yamada N, Higashi M, Kanzaki S, Hashimura H, Morita Y, Sakuma T, Noguchi T, Naito H, Sugimura K. Dynamic late gadolinium enhancement simply quantified using myocardium to lumen signal ratio: normal range of ratio and diffuse abnormal enhancement of cardiac amyloidosis. *J Magn Reson Imaging* 2011;**34**:50–55.
- Cerqueira MD, Weissman NJ, Dilsizian V, Jacobs AK, Kaul S, Laskey WK, Pennell DJ, Rumberger JA, Ryan T, Verani MS. Standardized myocardial segmentation and nomenclature for tomographic imaging of the heart: a statement for healthcare professionals from the Cardiac Imaging Committee of the Council on Clinical Cardiology of the American Heart Association. *Circulation* 2002;**105**:539–542.
- Holzmann M, Nicko A, Kuhl U, Noutsias M, Poller W, Hoffmann W, Morguet A, Witzensbichler B, Tschöpe C, Schultheiss HP, Pauschinger M. Complication rate of right ventricular endomyocardial biopsy via the femoral approach: a retrospective and prospective study analyzing 3048 diagnostic procedures over an 11-year period. *Circulation* 2008;**118**:1722–1728.
- Cunningham KS. An approach to endomyocardial biopsy interpretation. *J Clin Pathol* 2006;**59**:121–129.
- Karamitsos TD, Francis JM, Myerson S, Selvanayagam JB, Neubauer S. The role of cardiovascular magnetic resonance imaging in heart failure. *J Am Coll Cardiol* 2009;**54**:1407–1424.
- Patel MR, Cawley PJ, Heitner JF, Klem I, Parker MA, Jaroudi WA, Meine TJ, White JB, Elliott MD, Kim HW, Judd RM, Kim RJ. Detection of myocardial damage in patients with sarcoidosis. *Circulation* 2009;**120**:1969–1977.
- Vogelsberg H, Mahrholdt H, Deluigi CC, Yilmaz A, Kispert EM, Greulich S, Klingel K, Kandolf R, Sechtem U. Cardiovascular magnetic resonance in clinically suspected cardiac amyloidosis: noninvasive imaging compared to endomyocardial biopsy. *J Am Coll Cardiol* 2008;**51**:1022–1030.
- Abdel-Aty H, Boye P, Zagrosek A, Wassmuth R, Kumar A, Messroghli D, Bock P, Dietz R, Friedrich MG, Schulz-Menger J. Diagnostic performance of cardiovascular magnetic resonance in patients with suspected acute myocarditis: comparison of different approaches. *J Am Coll Cardiol* 2005;**45**:1815–1822.
- McCrohon JA, Moon JC, Prasad SK, McKenna WJ, Lorenz CH, Coats AJ, Pennell DJ. Differentiation of heart failure related to dilated cardiomyopathy and coronary artery disease using gadolinium-enhanced cardiovascular magnetic resonance. *Circulation* 2003;**108**:54–59.
- Magnani JW, Dec GW. Myocarditis: current trends in diagnosis and treatment. *Circulation* 2006;**113**:876–890.
- Diagnostic standard and guidelines for sarcoidosis. *Jpn J Sarcoidosis Granulomatous Disord* 2006;**26**:77–82. [in Japanese]
- Hughes SE. The pathology of hypertrophic cardiomyopathy. *Histopathology* 2004;**44**:412–427.
- Gradman AH, Alfayoumi F. From left ventricular hypertrophy to congestive heart failure: management of hypertensive heart disease. *Prog Cardiovasc Dis* 2006;**48**:326–341.
- JCS Joint Working Group. Guidelines for diagnosis and treatment of myocarditis (JCS 2009): digest version. *Circ J* 2011;**75**:734–743.
- Zimmermann O, Grebe O, Merkle N, Nusser T, Kochs M, Bienek-Ziolkowski M, Hombach V, Torzewski J. Myocardial biopsy findings and gadolinium enhanced cardiovascular magnetic resonance in dilated cardiomyopathy. *Eur J Heart Fail* 2006;**8**:162–166.
- Biagini E, Cocollo F, Ferlito M, Perugini E, Rocchi G, Bacchi-Reggiani L, Lofiego C, Boriani G, Prandstraller D, Picchio FM, Branzi A, Rapezzi C. Dilated-hypokinetic evolution of hypertrophic cardiomyopathy: prevalence, incidence, risk factors, and prognostic implications in pediatric and adult patients. *J Am Coll Cardiol* 2005;**46**:1543–1550.
- Harris KM, Spirito P, Maron MS, Zenovich AG, Formisano F, Lesser JR, Mackey-Bojack S, Manning WJ, Udelson JE, Maron BJ. Prevalence, clinical profile, and significance of left ventricular remodeling in the end-stage phase of hypertrophic cardiomyopathy. *Circulation* 2006;**114**:216–225.
- Cooper LT, Baughman KL, Feldman AM, Frustaci A, Jessup M, Kuhl U, Levine GN, Narula J, Starling RC, Towbin J, Virmani R. The role of endomyocardial biopsy in the management of cardiovascular disease: a scientific statement from the American Heart Association, the American College of Cardiology, and the European Society of Cardiology Endorsed by the Heart Failure Society of America and the Heart Failure Association of the European Society of Cardiology. *Eur Heart J* 2007;**28**:3076–3093.
- Hunt SA, Abraham WT, Chin MH, Feldman AM, Francis GS, Ganiats TG, Jessup M, Konstam MA, Mancini DM, Michl K, Oates JA, Rahko PS, Silver MA, Stevenson LW, Yancy CW. 2009 focused update incorporated into the ACC/AHA 2005 Guidelines for the Diagnosis and Management of Heart Failure in Adults: a report of the American College of Cardiology Foundation/American Heart Association Task Force on Practice Guidelines: developed in collaboration with the International Society for Heart and Lung Transplantation. *Circulation* 2009;**119**:e391–e479.
- Wu LA, Lapeyre AC 3rd, Cooper LT. Current role of endomyocardial biopsy in the management of dilated cardiomyopathy and myocarditis. *Mayo Clin Proc* 2001;**76**:1030–1038.
- Ardehali H, Howard DL, Hariri A, Qasim A, Hare JM, Baughman KL, Kasper EK. A positive endomyocardial biopsy result for sarcoid is associated with poor prognosis in patients with initially unexplained cardiomyopathy. *Am Heart J* 2005;**150**:459–463.
- Basso C, Ronco F, Marcus F, Abudurehman A, Rizzo S, Frigo AC, Baucé B, Maddalena F, Nava A, Corrado D, Grigoletto F, Thiene G. Quantitative assessment of endomyocardial biopsy in arrhythmogenic right ventricular cardiomyopathy/dysplasia: an *in vitro* validation of diagnostic criteria. *Eur Heart J* 2008;**29**:2760–2771.
- Bruder O, Schneider S, Nothnagel D, Dill T, Hombach V, Schulz-Menger J, Nagel E, Lombardi M, van Rossum AC, Wagner A, Schwitzer J, Senges J, Sabin GV, Sechtem U, Mahrholdt H. EuroCMR (European Cardiovascular Magnetic Resonance) registry: results of the German pilot phase. *J Am Coll Cardiol* 2009;**54**:1457–1466.
- Hansen MW, Merchant N. MRI of hypertrophic cardiomyopathy: part 2, differential diagnosis, risk stratification, and posttreatment MRI appearances. *AJR Am J Roentgenol* 2007;**189**:1344–1352.
- Rickers C, Wilke NM, Jerosch-Herold M, Casey SA, Panse P, Panse N, Weil J, Zenovich AG, Maron BJ. Utility of cardiac magnetic resonance imaging in the diagnosis of hypertrophic cardiomyopathy. *Circulation* 2005;**112**:855–861.
- Moon JC, Fisher NG, McKenna WJ, Pennell DJ. Detection of apical hypertrophic cardiomyopathy by cardiovascular magnetic resonance in patients with non-diagnostic echocardiography. *Heart* 2004;**90**:645–649.
- Mavrogeni S, Spargias C, Bratis C, Kolovou G, Markussis V, Papadopoulou E, Constadoulakis P, Papadimitropoulos M, Douskou M, Pavlides G, Cokkinos D. Myocarditis as a precipitating factor for heart failure: evaluation and 1-year follow-up using cardiovascular magnetic resonance and endomyocardial biopsy. *Eur J Heart Fail* 2011;**13**:830–837.
- Ardehali H, Qasim A, Cappola T, Howard D, Hruban R, Hare JM, Baughman KL, Kasper EK. Endomyocardial biopsy plays a role in diagnosing patients with unexplained cardiomyopathy. *Am Heart J* 2004;**147**:919–923.
- Friedrich MG, Sechtem U, Schulz-Menger J, Holmvang G, Alakija P, Cooper LT, White JA, Abdel-Aty H, Gutberlet M, Prasad S, Aletras A, Laissy JP, Paterson I, Filipchuk NG, Kumar A, Pauschinger M, Liu P. Cardiovascular magnetic resonance in myocarditis: a JACC White Paper. *J Am Coll Cardiol* 2009;**53**:1475–1487.

## Dipeptidyl-peptidase IV inhibition improves pathophysiology of heart failure and increases survival rate in pressure-overloaded mice

Ayako Takahashi,<sup>1,4</sup> Masanori Asakura,<sup>2</sup> Shin Ito,<sup>1</sup> Kyung-Duk Min,<sup>1</sup> Kazuhiro Shindo,<sup>1,4</sup> Yi Yan,<sup>4</sup> Yulin Liao,<sup>6</sup> Satoru Yamazaki,<sup>1</sup> Shoji Sanada,<sup>5</sup> Yoshihiro Asano,<sup>4,5</sup> Hatsue Ishibashi-Ueda,<sup>3</sup> Seiji Takashima,<sup>4,5</sup> Tetsuo Minamino,<sup>5</sup> Hiroshi Asanuma,<sup>7</sup> Naoki Mochizuki,<sup>1</sup> and Masafumi Kitakaze<sup>2</sup>

<sup>1</sup>Department of Cell Biology, <sup>2</sup>Department of Clinical Research and Development, and <sup>3</sup>Division of Pathology, National Cerebral and Cardiovascular Center, Osaka, Japan; <sup>4</sup>Department of Molecular Cardiology and <sup>5</sup>Department of Cardiovascular Medicine, Osaka University Graduate School of Medicine, Osaka, Japan; <sup>6</sup>Department of Cardiology, Nanfang Hospital, Southern Medical University, Guangzhou, China; and <sup>7</sup>Department of Cardiology, Kyoto Prefectural University School of Medicine, Kyoto, Japan

Submitted 12 June 2012; accepted in final form 25 January 2013

Takahashi A, Asakura M, Ito S, Min KD, Shindo K, Yan Y, Liao Y, Yamazaki S, Sanada S, Asano Y, Ishibashi-Ueda H, Takashima S, Minamino T, Asanuma H, Mochizuki N, Kitakaze M. Dipeptidyl-peptidase IV inhibition improves pathophysiology of heart failure and increases survival rate in pressure-overloaded mice. *Am J Physiol Heart Circ Physiol* 304: H1361–H1369, 2013. First published March 15, 2013; doi:10.1152/ajpheart.00454.2012.—Incretin hormones, including glucagon-like peptide-1 (GLP-1), a target for diabetes mellitus (DM) treatment, are associated with cardioprotection. As dipeptidyl-peptidase IV (DPP-IV) inhibition increases plasma GLP-1 levels in vivo, we investigated the cardioprotective effects of the DPP-IV inhibitor vildagliptin in a murine heart failure (HF) model. We induced transverse aortic constriction (TAC) in C57BL/6J mice, simulating pressure-overloaded cardiac hypertrophy and HF. TAC or sham-operated mice were treated with or without vildagliptin. An intraperitoneal glucose tolerance test revealed that blood glucose levels were higher in the TAC than in sham-operated mice, and these levels improved with vildagliptin administration in both groups. Vildagliptin increased plasma GLP-1 levels in the TAC mice and ameliorated TAC-induced left ventricular enlargement and dysfunction. Vildagliptin palliated both myocardial apoptosis and fibrosis in TAC mice, demonstrated by histological, gene and protein expression analyses, and improved survival rate on *day 28* (TAC with vildagliptin, 67.5%; TAC without vildagliptin, 41.5%;  $P < 0.05$ ). Vildagliptin improved cardiac dysfunction and overall survival in the TAC mice, both by improving impaired glucose tolerance and by increasing GLP-1 levels. DPP-IV inhibitors represent a candidate treatment for HF patients with or without DM.

heart failure; impaired glucose tolerance; dipeptidyl-peptidase IV inhibitor

HEART FAILURE (HF) is a leading cause of death in humans worldwide (1, 20, 37, 56), and is often linked to impaired glucose tolerance or diabetes mellitus (DM) (21, 53). DM is a major risk factor for cardiac dysfunction; Lind et al. (28) reported that poor glycemic control among patients with type 1 DM led to a high incidence of cardiovascular events. The energetic substrate utilization of cardiomyocytes under hyperglycemic conditions shifts from glucose to fatty acid oxidation, leading to HF (38). In DM, oxidative stress also causes endothelial dysfunction and decreases endothelial NO release, in-

ducing microangiopathy (13, 31). Either glucose abnormalities or diabetes commonly exists in patients with HF, but as previously reported, patients with diabetes have no worse outcome of HF (50). Our previous clinical study revealed that ~90% of patients with chronic HF had impaired glucose tolerance (21).

Incretin hormones have recently been proposed as new targets for DM treatment. Glucagon-like peptide-1 (GLP-1) is an incretin hormone secreted from the lower intestines and colon, which stimulates insulin secretion from pancreatic beta cells. Its receptors are ubiquitously expressed, including in the cardiovascular system (8). GLP-1 is thought to possess cardioprotective properties because of the following three reasons: 1) GLP-1 receptors localize to cardiomyocytes and endothelial cells (3, 57); 2) activation of GLP-1 receptors increases phosphoinositide 3 (PI3)-kinase, serine/threonine protein kinase Akt (Akt), and extracellular signal-regulated kinase phosphorylation, potentially mediating cardioprotection (6, 19); and 3) activation of GLP-1 receptors stimulates p38 mitogen-activated protein (MAP) kinase and endothelial nitric oxide synthase via protein kinase A activation, putatively affecting cardioprotection (5, 59) and plasma glucose normalization (16). As dipeptidyl-peptidase IV (DPP-IV) rapidly degrades GLP-1, which has a biological half-life of approximately 1.5–5 min (11, 18), both GLP-1 analogs and DPP-IV inhibitors have been developed as new drugs to treat type 2 DM. GLP-1 analogs reportedly ameliorate not only DM but also HF and myocardial ischemia (15, 33, 34, 48, 59), suggesting that DPP-IV inhibitors function cardioprotectively. Indeed, DPP-IV inhibitors are reportedly effective against myocardial infarction in mice and pacing-induced heart failure in pigs (14, 42, 59), suggesting that DPP-IV inhibitors may also affect the survival rate. However, the effects of DPP-IV inhibitors on the pathophysiology of pressure-overloaded HF and survival after HF are unknown.

We aimed to clarify whether vildagliptin, a DPP-IV inhibitor, improves the pathophysiology of HF and increases survival rate in pressure-overloaded mice.

### METHODS

All of the animal care procedures were performed according to the American Physiological Society “Guiding Principles in the Care and Use of Vertebrate Animals in Research and Training” and with the approval of the ethical committee of Osaka University.

Address for reprint requests and other correspondence: M. Asakura, Dept. of Clinical Research and Development, National Cerebral and Cardiovascular Center, 5-7-1, Fujishirodai, Suita, Osaka, 565-8565 Japan (e-mail: masakura@ncvc.go.jp).